Séminaire Poincaré XIV (2010) 177 – 220

Séminaire Poincaré

Anatomy of quantum chaotic eigenstates

Stéphane Nonnenmacher*
Institut de Physique Théorique
CEA-Saclay
91191 Gif-sur-Yvette, France

1 Introduction

These notes present a description of *quantum chaotic eigenstates*, that is bound states of quantum dynamical systems, whose classical limit is chaotic. The classical dynamical systems we will be dealing with are mostly of two types: geodesic flows on Euclidean domains ("billiards") or compact riemannian manifolds, and canonical transformations on a compact phase space; the common feature is the "chaoticity" of the dynamics. The corresponding quantum systems will always be considered within the semiclassical (or high-frequency) régime, in order to establish a connection them with the classical dynamics. As a first illustration, we plot below two eigenstates of a paradigmatic system, the Laplacian on the *stadium billiard*, with Dirichlet boundary conditions[1].

The study of chaotic eigenstates makes up a large part of the field of *quantum chaos*. It is somewhat complementary with the contribution of J. Keating (who will focus on the statistical properties of quantum spectra, another major topic in quantum chaos). I do not include the study of eigenstates of quantum graphs (a recent interesting development in the field), since this question should be addressed in U.Smilansky's lecture. Although these notes are purely theoretical, H.-J. Stöckmann's lecture will show that the questions raised have direct experimental applications (his lecture should present experimentally measured eigenmodes of 2- and 3-dimensional "billiards").

One common feature of the chaotic eigenfunctions (except in some very specific systems) is the absence of explicit, or even approximate, formulas. One then has to resort to indirect, rather unprecise approaches to describe these eigenstates. We will use various analytic tools or points of view: deterministic/statistical, macro/microscopic, pointwise/global properties, generic/specific systems. The level of rigour in the results varies from mathematical proofs to heuristics, generally supported by numerical experiments. The necessary selection of results reflects my personal view or knowledge of the subject, it omits several important developments, and is more "historical" than sharply up-to-date. The list of references is thick, but in no way exhaustive.

*I am grateful to E.Bogomolny, who allowed me to reproduce several plots from [26]. The author has been partially supported by the Agence Nationale de la Recherche under the grant ANR-09-JCJC-0099-01. These notes were written while he was visiting the Institute of Advanced Study in Princeton, supported by the National Science Foundation under agreement No. DMS-0635607.

[1]The eigenfunctions of the stadium plotted in this article were computed using a code nicely provided to me by E. Vergini, which uses the *scaling method* invented in [94].

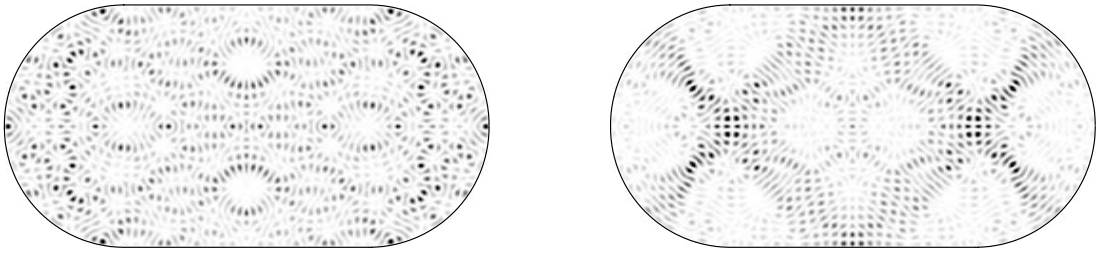

Figure 1: Two eigenfunctions of the Dirichlet Laplacian in the stadium billiard, with wavevectors $k = 60.196$ and $k = 60.220$ (see (9)). Large values of $|\psi(x)|^2$ correspond to dark regions, while nodal lines are white. While the left eigenfunction looks relatively "ergodic", the right one is *scarred* by two symmetric periodic orbits (see §4.2).

These notes are organized as follows. We introduce in section 2 the classical dynamical systems we will focus on (mostly geodesic flows and maps on the 2-dimensional torus), mentioning their degree of "chaos". We also sketch the quantization procedures leading to quantum Hamiltonians or propagators, whose eigenstates we want to understand. We also mention some properties of the semiclassical/high-frequency limit. In section 3 we describe the *macroscopic* properties of the eigenstates in the semiclassical limit, embodied by their *semiclassical measures*. These properties include the *quantum ergodicity* property, which for some systems (with arithmetic symmetries) can be improved to quantum *unique* ergodicity, namely the fact that all high-frequency eigenstates are "flat" at the macroscopic scale; on the opposite, some specific systems allow the presence of exceptionally localized eigenstates. In section 4 we focus on more refined properties of the eigenstates, many of *statistical* nature (value distribution, correlation functions). Very little is known rigorously, so one has to resort to models of *random wavefunctions* to describe these statistical properties. The large values of the wavefunctions or Husimi densities are discussed, including the *scar phenomenon*. Section 5 discusses the most "quantum" or microscopic aspect of the eigenstates, namely their *nodal sets*, both in position and phase space (Husimi) representations. Here as well, the random state models are helpful, and lead to interesting questions in probability theory.

2 What is a quantum chaotic eigenstate?

In this section we first present a general definition of the notion of "chaotic eigenstates". We then focus our attention to geodesic flows on Euclidean domains or on compact riemannian manifolds, which form the simplest systems proved to be chaotic. Finally we present some discrete time dynamics (chaotic canonical maps on the 2-dimensional torus).

2.1 A short review of quantum mechanics

Let us start by recalling that classical mechanics on the phase space $T^*\mathbb{R}^d$ can be defined, in the Hamiltonian formalism, by a real valued function $H(x,p)$ on that phase space, called the Hamiltonian. We will always assume the system to be autonomous, namely the function H to be independent of time. This function then

generates the flow[2]

$$(x(t), p(t)) = \Phi_H^t(x(0), p(0)), \qquad t \in \mathbb{R}\,,$$

by solving Hamilton's equations:

$$\dot{x}_j(t) = \frac{\partial H}{\partial p_j}(x(t), p(t)), \quad \dot{p}_j = -\frac{\partial H}{\partial x_j}(x(t), p(t)). \tag{1}$$

This flow preserves the symplectic form $\sum_j dp_j \wedge dx_j$, and the energy shells $\mathcal{E}_E = H^{-1}(E)$.

The corresponding quantum mechanical system is defined by an operator $\hat{H}_\hbar$ acting on the (quantum) Hilbert space $\mathcal{H} = L^2(\mathbb{R}^d, dx)$. This operator can be formally obtained by replacing coordinates x, p by operators:

$$\hat{H}_\hbar = H(\hat{x}_\hbar, \hat{p}_\hbar), \tag{2}$$

where $\hat{x}_\hbar$ is the operator of multiplication by x, while the momentum operator $\hat{p}_\hbar = \frac{\hbar}{i}\nabla$, is conjugate to $\hat{x}$ through the $\hbar$-Fourier transform $\mathcal{F}_\hbar$. The notation (2) assumes that one has selected a certain ordering between the operators $\hat{x}_\hbar$ and $\hat{p}_\hbar$; in physics one usually chooses the fully symmetric ordering, also called the *Weyl quantization*: it has the advantage to make $\hat{H}_\hbar$ a self-adjoint operator on $L^2(\mathbb{R}^d)$. Quantization procedures can also be defined when the Euclidean space $\mathbb{R}^d$ is replaced by a compact manifold M. We will not describe it in any detail.

The quantum dynamics, which governs the evolution of the wavefunction $\psi(t) \in \mathcal{H}$ describing the system, is then given by the Schrödinger equation:

$$i\hbar\,\frac{\partial \psi(x,t)}{\partial t} = [\hat{H}_\hbar\,\psi](x,t)\,. \tag{3}$$

Solving this linear equation produces the propagator, that is the family of unitary operators on $L^2(\mathbb{R}^d)$,

$$U_\hbar^t = \exp(-i\hat{H}_\hbar/\hbar)\,, \quad t \in \mathbb{R}\,.$$

Remark 1 *In physical systems, Planck's constant $\hbar$ is a fixed number, which is of order 10^{-34} in SI units. However, if the system (atom, molecule, "quantum dot") is itself microscopic, the value of $\hbar$ may be comparable with the* typical action *of the system, in which case it is more natural to select units in which $\hbar = 1$. Our point of view throughout this work will be the opposite: we will assume that $\hbar$ is (very) small compared with the typical action of the system, and many results will be valid asymptotically, in the* semiclassical limit $\hbar \to 0$.

2.2 Quantum-classical correspondence

At this point, let us introduce the crucial semiclassical property of the quantum evolution: it is called (in the physics literature) the quantum-classical correspondence, while in mathematics this result is known as Egorov's theorem. This property states that the evolution of observables approximately commutes with their quantization. For us, an observable is a smooth, compactly supported function on phase space

[2]We always assume that the flow is complete, that is it does not blow up in finite time.

$f \in C_c^\infty(T^*\mathbb{R}^d)$. The evolution of classical and quantum evolutions are defined by duality with that of particles/wavefunctions:

$$f(t) = f \circ \Phi_H^t, \qquad \hat{f}_\hbar(t) = U_\hbar^{-t} \hat{f}_\hbar U_\hbar^t .$$

The quantum-classical correspondence connects these two evolutions:

$$\forall t \in \mathbb{R}, \qquad f_\hbar(t) = \widehat{f(t)}_\hbar + \mathcal{O}(e^{\Gamma|t|}\hbar) , \tag{4}$$

where the exponent $\Gamma > 0$ depends on the flow and on the observable f.

The most common form of dynamics is the motion of a scalar particle in an electric potential $V(x)$. It corresponds to the Hamiltonian

$$H(x,p) = \frac{|p|^2}{2m} + qV(x), \quad \text{quantized into} \quad \hat{H}_\hbar = -\frac{\hbar^2\Delta}{2m} + qV(x) . \tag{5}$$

We will usually scale the mass and electric charge to $m = q = 1$, keeping $\hbar$ small. Since the Hamilton flow (1) leaves each energy energy shell $\mathcal{E}_E$ invariant, we may restrict our attention to the flow on a single shell. We will be interested in cases where

1. the energy shell $\mathcal{E}_E$ is *bounded* in phase space (that is, both the positions and momenta of the particles remain finite at all times). This is the case if $V(x)$ is confining ($V(x) \to \infty$ as $|x| \to \infty$).
2. the flow on $\mathcal{E}_E$ is *chaotic* (and this is also the case on the neighbouring shells $\mathcal{E}_{E+\epsilon}$). "Chaos" is a vague word, which we will make more precise below.

The first condition implies that, provided $\hbar$ is small enough, the spectrum of $\hat{H}_\hbar$ is purely discrete near the energy E, with eigenstates $\psi_{\hbar,j} \in L^2(\mathbb{R}^d)$ (*bound states*). Besides, fixing some small $\epsilon > 0$ and letting $\hbar \to 0$, the number of eigenstates of $\hat{H}_\hbar$ with eigenvalues $E_{\hbar,j} \in [E-\epsilon, E+\epsilon]$ typically grows like $C\hbar^{-d}$. Under the second condition, the eigenstates with energies in this interval can be called *quantum chaotic eigenstates*.

Below we describe several degrees of "chaos", which regard the *long time properties* of the classical flow. These properties are relevant when describing the eigenstates of the quantum system, which form the "backbone" of the long time quantum dynamics. The main objective of quantum chaos consists in connecting, in a precise way, the classical and quantum long time (or time independent) properties.

2.3 Various levels of chaos

For most Hamiltonians of the form (5) (e.g. the physically relevant case of a hydrogen atom in a constant magnetic field), the classical dynamics on bounded energy shells $\mathcal{E}_E$ involves both regular and chaotic regions of phase space; one then speaks of a *mixed dynamics* on $\mathcal{E}_E$. The regular region is composed of a number of "islands of stability", made of quasiperiodic motion structured around stable periodic orbits; these islands are embedded in a "chaotic sea" where trajectories are unstable (they have a positive Lyapunov exponent). These notions of "island of stability" versus "chaotic sea" are rather poorly understood mathematically, but have received compelling numerical evidence [68]. The main conjecture concerning the corresponding

quantum system, is that most eigenstates are either localized in the regular region, or in the chaotic sea [80]. To my knowledge this conjecture remains fully open at present, in part due to our lack of understanding of the classical dynamics.

For this reason, I will restrict myself (as most researches in quantum chaos do) to the case of systems admitting a *purely chaotic* dynamics on $\mathcal{E}_E$. I will allow various degrees of chaos, the minimal assumption being the *ergodicity* of the flow Φ_H^t on $\mathcal{E}_E$, with respect to the natural (Liouville) measure on $\mathcal{E}_E$. This assumption means that, for almost any initial position $\mathbf{x}_0 \in \mathcal{E}_E$, the time averages of any observable f converge to its phase space average:

$$\lim_{T\to\infty} \frac{1}{2T} \int_{-T}^{T} f(\Phi^t(\mathbf{x}_0))\, dt = \int_{\mathcal{E}_E} f(\mathbf{x})\, d\mu_L(\mathbf{x}) \stackrel{\text{def}}{=} \int f(\mathbf{x})\, \delta(H(\mathbf{x}) - E)\, d\mathbf{x}\,. \qquad (6)$$

A stronger chaotic property is the *mixing* property, or decay of time correlations between two observables f, g:

$$C_{f,g}(t) \stackrel{\text{def}}{=} \int_{\mathcal{E}_E} g \times (f \circ \Phi^t)\, d\mu_L - \int f\, d\mu_L \int g\, d\mu_L \xrightarrow{t\to\infty} 0\,. \qquad (7)$$

The rate of mixing depends on both the flow Φ^t and the regularity of the observables f, g. For very chaotic flows (Anosov flows, see §2.4.2) and smooth observables, the decay is exponential.

2.4 Geometric quantum chaos

In this section we give explicit examples of chaotic flows, namely geodesic flows in a Euclidean billiard, or on a compact manifold. The dynamics is then induced by the geometry, rather than a potential. Both the classical and quantum properties of these systems have been investigated a lot in the past 30 years.

2.4.1 Billiards

The simplest form of ergodic system occurs when the potential $V(x)$ is an infinite barrier delimiting a bounded domain $\Omega \subset \mathbb{R}^d$ (say, with piecewise smooth boundary), so that the particle moves freely inside Ω and bounces specularly at the boundaries. For obvious reasons, such a system is called a *Euclidean billiard*. All positive energy shells are equivalent to one another, up to a rescaling of the velocity, so we may restrict our attention to the shell $\mathcal{E} = \{(x, p),\, x \in \Omega,\, |p| = 1\}$. The long time dynamical properties only depend on the shape of the domain. For instance, in 2 dimensions, a rectangular, circular or elliptic billiards lead to an *integrable* dynamics: the flow admits two independent integrals of motion — in the case of the circle, the energy and the angular momentum. A convex billiard with a smooth boundary will always admit some stable "whispering gallery" stable orbits. On the opposite, the famous *stadium billiard* (see Fig. 2) was proved to be ergodic by Bunimovich [32]. Historically, the first Euclidean billiard proved to be ergodic was the Sinai billiard, composed of one or several circular obstacles inside a square (or torus) [91]. These billiards also have positive Lyapunov exponents (meaning that almost all trajectories are exponentially unstable, see the left part of Fig. 2). It has been shown more recently that these billiards are *mixing*, but with correlations decaying at polynomial or subexponential rates [34, 14, 73].

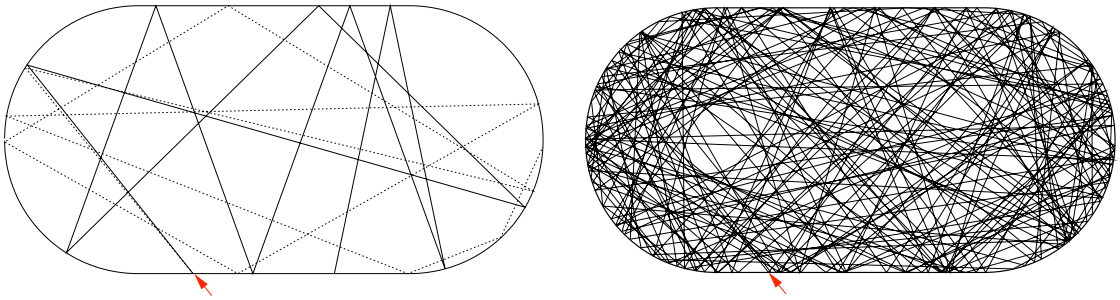

Figure 2: Left: two trajectories in the stadium billiard, initially very close to one another, and then diverging fast (the red arrow shows the initial point). Right: long evolution of one of the trajectories.

The quantization of the broken geodesic flow inside Ω is the (semiclassical) Laplacian with Dirichlet boundary conditions:

$$\hat{H}_\hbar = -\frac{\hbar^2 \Delta_\Omega}{2} \,. \tag{8}$$

Obviously, the parameter $\hbar$ only amounts to a rescaling of the spectrum: an eigenstate $\psi_\hbar$ of (8) with energy $E_\hbar \approx 1/2$ is also an eigenstate of $-\Delta_\Omega$ with eigenvalue $k^2 \approx \hbar^{-2}$. Hence, $\hbar$ represents the *wavelength* of $\psi_\hbar$, the inverse of its *wavevector* k. Fixing $E = 1/2$ and taking the semiclassical limit $\hbar \to 0$ is equivalent with studying the high-frequency or high-wavevector spectrum of $-\Delta_\Omega$.

The system (8) is often called a *quantum billiard*, although this operator is not only relevant in quantum mechanics, but in all sorts of wave mechanics (see H.-J. Stöckmann's lecture). Indeed, the scalar Helmholtz equation

$$\Delta \psi_j + k_j^2 \psi_j = 0 \,, \tag{9}$$

may describe stationary acoustic waves in a cavity. This equation is also relevant to describe electromagnetic waves in a quasi-2D cavity, provided one is allowed to separate the different polarization components of the electric field.

Euclidean billiards thus form the simplest *realistic* quantized chaotic systems, for which the classical dynamics is well understood at the mathematical level. Besides, the spectrum of the Dirichlet Laplacian can be numerically computed up to large values of k using methods specific to the Euclidean geometry, like the scaling method [94]. For these reasons, these billiards have become a paradigm of quantum chaos studies.

2.4.2 Anosov geodesic flows

The strongest form of chaos occurs in systems (maps or flows) with the *Anosov property*, also called *uniformly hyperbolic systems* [5]. The first (and main) example of an Anosov flow is given by the *geodesic flow on a compact riemannian manifold* (M, g) *of negative curvature*, generated by the free particle Hamiltonian $H(x, p) = |p|_g^2/2$. Uniform hyperbolicity — which is induced by the negative curvature of the manifold — means that at each point $\mathbf{x} \in \mathcal{E}$ the tangent space $T_\mathbf{x}\mathcal{E}$ splits into the vector $X_\mathbf{x}$ generating the flow, the unstable subspace $E^+_\mathbf{x}$ and the stable subspace

$E^-_{\mathbf{x}}$. The stable (resp. unstable) subspace is defined by the property that the flow contracts vectors exponentially in the future (resp. in the past), see Fig. 3:

$$\forall v \in E^{\pm}_{\mathbf{x}}, \forall t > 0, \quad \|d\Phi^{\mp t}_{\mathbf{x}} \cdot v\| \leq C\, e^{-\lambda t} \|v\|. \tag{10}$$

Anosov systems present the strongest form of chaos, but their ergodic properties are (paradoxically) better understood than for the billiards of the previous section. The flow has a positive *complexity*, reflected in the exponential proliferation of long periodic geodesics.

For this reason, this geometric model has been at the center of the mathematical investigations of quantum chaos, in spite of its minor physical relevance. Generalizing

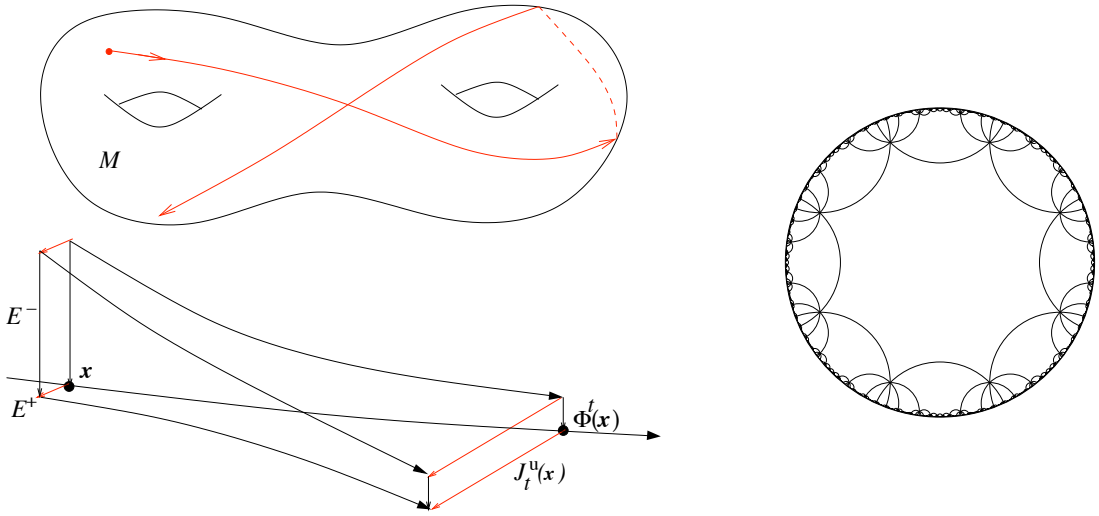

Figure 3: Top left: geodesic flow on a surface of negative curvature (such a surface have a genus ≥ 2). Right: fundamental domain for an "octagon" surface $\Gamma\backslash\mathbb{H}$ of constant negative curvature (the figure is due to C. McMullen) Botton left: a phase space trajectory and two nearby trajectories approaching it in the future or past. The stable/unstable directions at $\mathbf{x}$ and $\Phi^t(\mathbf{x})$ are shown. The red lines feature the expansion along the unstable direction, measured by the unstable Jacobian $J^u_t(\mathbf{x}) = \det(d\Phi^t \restriction_{E^+_{\mathbf{x}}})$.

the case of the Euclidean billiards, the quantization of the geodesic flow on $(M - g)$ is given by the (semiclassical) Laplace-Beltrami operator,

$$\hat{H}_\hbar = -\frac{\hbar^2 \Delta_g}{2}\,, \tag{11}$$

acting on the Hilbert space is $L^2(M, dx)$ associated with the Lebesgue measure. The eigenstates of $\hat{H}_\hbar$ with eigenvalues $\approx 1/2$ (equivalently, the high-frequency eigenstates of $-\Delta_g$) constitute a class of quantum chaotic eigenstates, whose study is not impeded by boundary problems present in billiards.

The spectral properties of this Laplacian have interested mathematicians working in riemannian geometry, PDEs, analytic number theory, representation theory, for at least a century, while the specific "quantum chaotic" aspects have emerged only in the last 30 years.

The first example of a manifold with negative curvature is the Poincaré half-space (or disk) $\mathbb{H}$ with its hyperbolic metric $\frac{dx^2+dy^2}{y^2}$, on which the group $SL_2(\mathbb{R})$

acts isometrically by Moebius transformations. For certain discrete subgroups Γ of $PSL_2(\mathbb{R})$ (called co-compact lattices), the quotient $M = \Gamma\backslash\mathbb{H}$ is a smooth compact surface. This group structure provides detailed information on the spectrum of the Laplacian (for instance, the Selberg trace formula explicitly connects the spectrum with the periodic geodesics of the geodesic flow).

Furthermore, for some of these discrete subgroups Γ, (called *arithmetic*), one can construct a commutative algebra of Hecke operators on $L^2(M)$, which also commute with the Laplacian; it then make sense to study in priority the joint eigenstates of Δ and of these Hecke operators, which we will call the Hecke eigenstates. This arithmetic structure provides nontrivial information on these eigenstates (see §3.3.3), so these eigenstates will appear several times along these notes. Their study composes a part of *arithmetic quantum chaos*, a lively field of research.

2.5 Classical and quantum chaotic maps

Beside the Hamiltonian or geodesic flows, another model system has attracted much attention in the dynamical systems community: chaotic maps on some compact phase space $\mathcal{P}$. Instead of a flow, the dynamics is given by a discrete time transformation $\kappa : \mathcal{P} \to \mathcal{P}$. Because we want to quantize these maps, we require the phase space $\mathcal{P}$ to have a symplectic structure, and the map κ to preserve this structure (in other words, κ is an invertible canonical transformation on $\mathcal{P}$.

The advantage of studying maps instead of flows is multifold. Firstly, a map can be easily constructed from a flow by considering a *Poincaré section* Σ transversal to the flow; the induced return map $\kappa_\Sigma : \Sigma \to \Sigma$, together with the return time, contain all the dynamical information on the flow. Ergodic properties of chaotic maps are usually easier to study than their flow counterpart. For billiards, the natural Poincaré map to consider is the boundary map κ_Σ defined on the phase space associated with the boundary, $T^*\partial\Omega$. The ergodic of this boundary map were understood, and used to address the case of the billiard flow itself [14].

Secondly, simple chaotic maps can be defined on low-dimensional phase spaces, the most famous ones being the hyperbolic symplectomorphisms on the 2-dimensional torus. These are defined by the action of a matrix $S = \begin{pmatrix} a & b \\ c & d \end{pmatrix}$ with integer entries, determinant unity and trace $a+d > 2$ (equivalently, S is unimodular and hyperbolic). Such a matrix obviously acts on $\mathbf{x} = (x, p) \in \mathbb{T}^2$ linearly, through

$$\kappa_S(\mathbf{x}) = (ax + bp, cx + dp) \bmod 1\,. \tag{12}$$

A schematic view of κ_S for the famous *Arnold's cat map* $S_{cat} = \begin{pmatrix} 1 & 1 \\ 1 & 2 \end{pmatrix}$ is shows in Fig. 5. The hyperbolicity condition implies that the eigenvalues of S are of the form $\{e^{\pm\lambda}\}$ for some $\lambda > 0$. As a result, κ_S has the Anosov property: at each point $\mathbf{x}$, the tangent space $T_{\mathbf{x}}\mathbb{T}^2$ splits into stable and unstable subspaces, identified with the eigenspaces of S, and $\pm\lambda$ are the Lyapunov exponents. Many dynamical properties of κ_S can be explicitly computed. For instance, every rational point $\mathbf{x} \in \mathbb{T}^2$ is periodic, and the number of periodic orbits of period $\leq n$ grows like $e^{\lambda n}$ (thus λ also measures the complexity of the map). This linearity also results in the fact that the decay of correlations (for smooth observables) is superexponential instead of exponential for a generic Anosov diffeomorphism. More generic Anosov diffeomorphisms of the

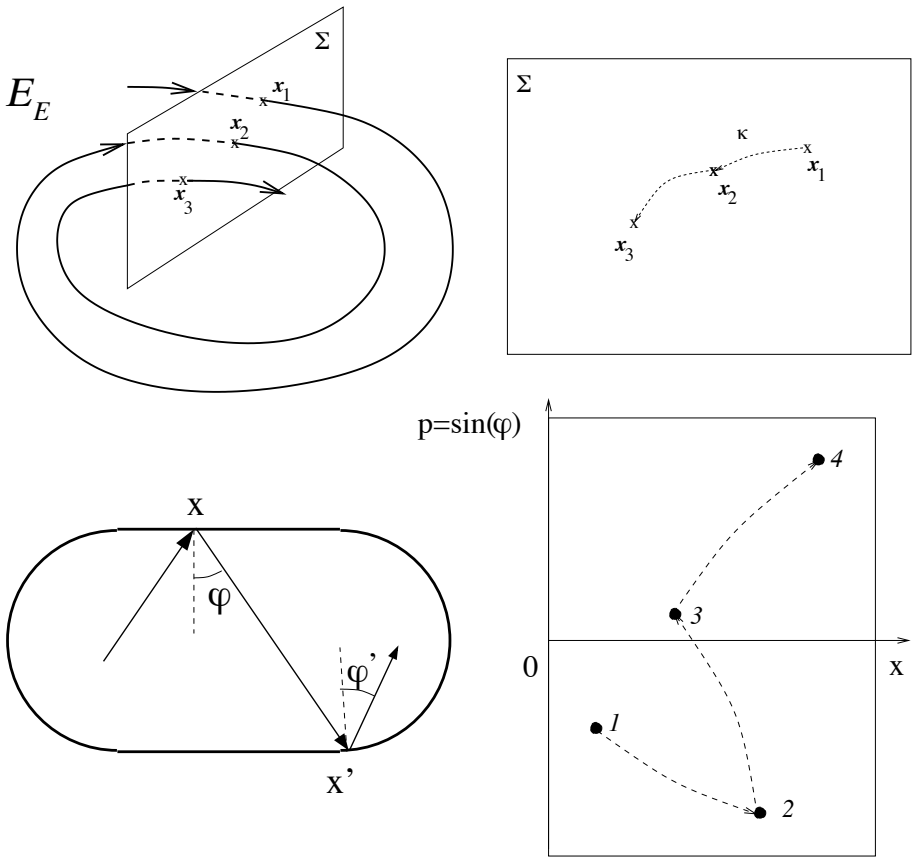

Figure 4: Top: Poincaré section and the associated return map constructed from a Hamiltonian flow on $\mathcal{E}_E$. Bottom: boundary map associated with the stadium billiard.

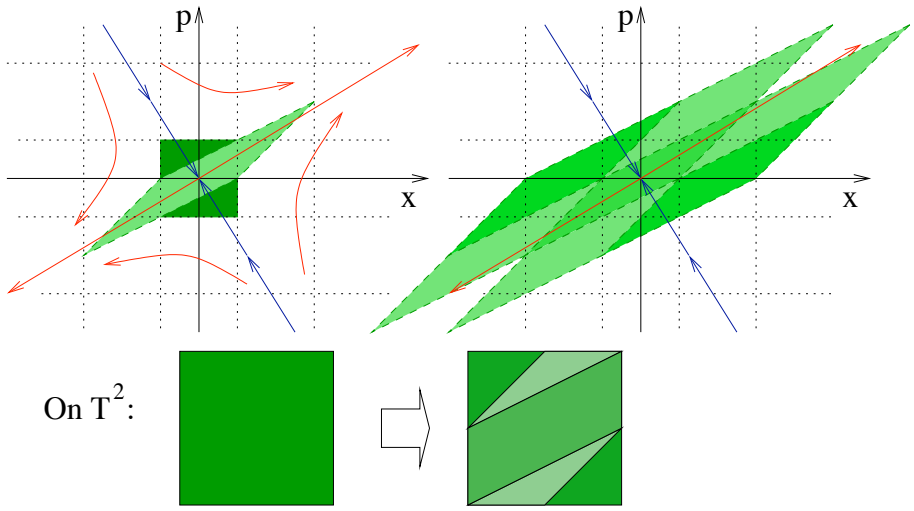

Figure 5: Construction of Arnold's cat map $\kappa_{S_{cat}}$ on the 2-torus, obtained by periodizing the linear transformation on $\mathbb{R}^2$. The stable/unstable directions are shown (kindly provided by F. Faure).

2-torus can be obtained by smoothly perturbing the linear map κ_S. Namely, for a given Hamiltonian $H \in C^\infty(\mathbb{T}^2)$, the composed map $\Phi_H^\epsilon \circ \kappa_S$ remains Anosov if ϵ is small enough, due to the structural stability of Anosov diffeomorphisms.

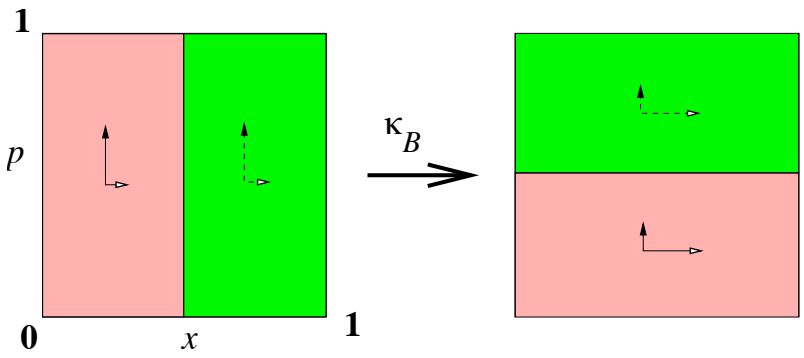

Figure 6: Schematic view of the baker's map (13). The arrows show the contraction/expansion directions.

Another family of canonical maps on the torus was also much investigated, namely the so-called *baker's maps*, which are piecewise linear. The simplest (symmetric) baker's map is defined by

$$\kappa_B(x,p) = \begin{cases} (2x \bmod 1, \frac{p}{2}), & 0 \le x < 1/2, \\ (2x \bmod 1, \frac{p+1}{2}), & 1/2 \le x < 1. \end{cases} \tag{13}$$

This map is conjugated to a very simple *symbolic dynamics*, namely the shift on two symbols. Indeed, if one considers the binary expansions of the coordinates $x = 0, \alpha_1\alpha_2\cdots$, $p = \beta_1\beta_2\cdots$, then the map $(x,p) \mapsto \kappa_B(x,p)$ equivalent with the shift to the left on the bi-infinite sequence $\cdots\beta_2\beta_1 \cdot \alpha_1\alpha_2\cdots$. This conjugacy allows to easily prove that the map is ergodic and mixing, identify all periodic orbits, and provide a large set of nontrivial invariant probability measures. All trajectories not meeting the discontinuity lines are uniformly hyperbolic.

Simple canonical maps have also be defined on the 2-sphere phase space (like the kicked top), but their chaotic properties have, to my knowledge, not been rigorously proven. Their quantization has been intensively investigated.

2.5.1 Quantum maps on the 2-dimensional torus

As opposed to the case of Hamiltonian flows, there is no natural rule to quantize a canonical map on a compact phase space $\mathcal{P}$. Already, associating a quantum Hilbert space to this phase space is not obvious. Therefore, from the very beginning, quantum maps have been defined through somewhat arbitrary (or rather, *ad hoc*) procedures, often specific to the considered map $\kappa : \mathcal{P} \to \mathcal{P}$. Still these recipes are always required to satisfy a certain number of properties:

- one needs a *sequence* of Hilbert spaces $(\mathcal{H}_N)_{N\in\mathbb{N}}$ of dimensions N. Here N is interpreted as the inverse of Planck's constant, in agreement with the heuristics that *each quantum state occupies a volume $\hbar^d$ in phase space*. We also want to quantize observables $f \in C(\mathcal{P})$ into hermitian operators $\hat{f}_N$ on $\mathcal{H}_N$.

- For each $N \geq 1$, the quantization of κ is given by a unitary propagator $U_N(\kappa)$ acting on $\mathcal{H}_N$. The whole family $(U_N(\kappa))_{N\geq 1}$ is called the quantum map associated with κ.
- in the semiclassical limit $N \sim \hbar^{-1} \to \infty$, this propagator satisfies some form of quantum-classical correspondence. Namely, for some (large enough) family of observables f on $\mathcal{P}$, we should have

$$\forall n \in \mathbb{Z}, \qquad U_N^{-n}\, \hat{f}_N\, U_N^n = \widehat{(f \circ \kappa^n)}_N + \mathcal{O}_n(N^{-1}) \qquad \text{as } N \to \infty. \tag{14}$$

The condition (14) is the analogue of the Egorov property (4) satisfied by the propagator $U_\hbar$ associated with a quantum Hamiltonian, which quantizes the stroboscopic map $\mathbf{x} \mapsto \Phi_H^1(\mathbf{x})$.

Let us briefly summarize the explicit construction of the quantizations $U_N(\kappa)$, for the maps $\kappa : \mathbb{T}^2 \to \mathbb{T}^2$ presented in the previous section. Let us start by constructing the quantum Hilbert space. One can see $\mathbb{T}^2$ as the quotient of the phase space $T^*\mathbb{R} = \mathbb{R}^2$ by the discrete translations $\mathbf{x} \mapsto \mathbf{x} + \mathbf{n}$, $\mathbf{n} \in \mathbb{Z}^2$. Hence, it is natural to construct quantum states on $\mathbb{T}^2$ by starting from states $\psi \in L^2(\mathbb{R})$, and requiring the following periodicity properties

$$\psi(x + n_1) = \psi(x), \quad (\mathcal{F}_\hbar\psi)(p + n_2) = (\mathcal{F}_\hbar\psi)(p), \quad n_1, n_2 \in \mathbb{Z}.$$

It turns out that these two conditions can be satisfied only if $\hbar = (2\pi N)^{-1}$, $N \in \mathbb{N}$, and the corresponding states (which are actually distributions) then form a vector space $\mathcal{H}_N$ of dimension N. A basis of this space is given by the Dirac combs

$$e_j(x) = \frac{1}{\sqrt{N}} \sum_{\nu\in\mathbb{Z}} \delta(x - \frac{j}{N} - \nu), \qquad j = 0, \ldots, N-1\,. \tag{15}$$

It is natural to equip $\mathcal{H}_N$ with the hermitian structure for which the basis $\{e_j,\, j = 0, \ldots, N-1\}$ is orthonormal.

Let us now explain how the linear symplectomorpisms κ_S are constructed [48]. Given a unimodular matrix S, its action on $\mathbb{R}^2$ can be generated by a quadratic polynomial $H_S(x, p)$; this action can thus be quantized into the unitary operator $U_\hbar(S) = \exp(-i\hat{H}_{S,\hbar}/\hbar)$ on $L^2(\mathbb{R})$. This operator also acts on distributions $\mathcal{S}'(\mathbb{R})$, and in particular on the finite subspace $\mathcal{H}_N$. Provided the matrix S satisfies some "checkerboard condition", one can show (using group theory) that the action of $U_\hbar(S)$ on $\mathcal{H}_N$ *preserves that space*, and acts on it through a unitary matrix $U_N(S)$. The family of matrices $(U_N(S))_{N\geq 1}$ defines the quantization of the map κ_S on $\mathbb{T}^2$. Group theory also implies that an *exact* quantum-classical correspondence holds (that is, the remainder term in (14) vanishes), and has other important consequences regarding the operators $U_N = U_N(\kappa_S)$ (for each N the matrix U_N is periodic, of period $T_N \leq 2N$). Explicit expressions for the coefficients matrices $U_N(S)$ can be worked out, they depends quite sensitively on the arithmetic properties of the dimension N.

The construction of the quantized baker's map (13) proceeds very differently. An Ansatz was proposed by Balasz-Voros [13], with the following form (we assume that N is an even integer):

$$U_N(\kappa_B) = F_N^* \begin{pmatrix} F_{N/2} & \\ & F_{N/2} \end{pmatrix}, \tag{16}$$

where F_N is the N-dimensional discrete Fourier transform. This Ansatz is obviously unitary. It was guided by the fact that the phases of the matrix elements of the block-diagonal matrix can be interpreted as the discretization of the generating function $S(p,x) = 2px$ for the map (13). A proof that the matrices $U_N(\kappa_B)$ satisfy the Egorov property (14) was given in [39].

Once we have constructed the matrices $U_N(\kappa)$ associated with a chaotic map κ, their eigenstates $\{\psi_{N,j},\ j = 1,\dots,N\}$ enjoy the rôle of quantum chaotic eigenstates. They are of quite different nature from the eigenstates of the Laplacian on a manifold or a billiard: while the latter belong to $L^2(M)$ or $L^2(\Omega)$ (and are actually smooth functions), the eigenstates $\psi_{N,j}$ are N-dimensional vectors. Still, part of "quantum chaos" has consisted in developing common tools to analyze these eigenstates, in spite of the different functional settings.

3 Macroscopic description of the eigenstates

In this section we will study the *macroscopic* localization properties of chaotic eigenstates. Most of the results are mathematically rigorous.

In the case of the semiclassical Laplacian (8) on a billiard Ω we will ask the following question:

> Consider a sequence $(\psi_\hbar)_{\hbar\to 0}$ of normalized eigenstates of $\hat{H}_\hbar$, with energies $E_\hbar \approx 1/2$. For $A \subset \Omega$ a fixed subdomain, what is the probability that the particle described by the stationary state $\psi_\hbar$ lies inside A? How do the probability weights $\int_A |\psi_\hbar(x)|^2\,dx$ behave when $\hbar \to 0$?

This question is quite natural, when contemplating eigenstate plots like in Fig. 1. Here, by macroscopic we mean that the domain A is kept fixed while $\hbar \to 0$.

One can obviously generalize the question to integrals of the type $\int_\Omega f(x)\,|\psi_\hbar(x)|^2\,dx$, with $f(x)$ a continuous test function on Ω. This integral can be interpreted as the matrix element $\langle\psi_\hbar|\hat{f}_\hbar|\psi_\hbar\rangle$, where the quantum observable $\hat{f}_\hbar$ is just the multiplication operator by $f(x)$. It proves useful to extend the question to phase space observables $f(x,p)$[3]: what is the behaviour of the diagonal matrix elements

$$\mu^W_{\psi_\hbar}(f) \stackrel{\text{def}}{=} \langle\psi_\hbar, \hat{f}_\hbar\psi_\hbar\rangle, \qquad f \in C^\infty(T^*\Omega)\,, \quad \text{in the limit } \hbar\to 0? \tag{17}$$

Since the quantization procedure $f \mapsto \hat{f}_\hbar$ is linear, these matrix elements define a distribution $\mu^W_{\psi_\hbar} = W_{\psi_\hbar}(\mathbf{x})\,d\mathbf{x}$ in $T^*\Omega$, called the Wigner distribution of the state $\psi_\hbar$ (the density $W_{\psi_\hbar}(\mathbf{x})$ called the Wigner function). Although this function is generally not positive, it is interpreted as a quasi-probability density describing the state $\psi_\hbar$ in *phase space*.

On the Euclidean space, one can define a *nonnegative* phase space density associated to the state $\psi_\hbar$: the *Husimi* measure (and function):

$$\mu^H_{\psi_\hbar} = \mathcal{H}_{\psi_\hbar}(\mathbf{x})\,d\mathbf{x}, \qquad \mathcal{H}_{\psi_\hbar}(\mathbf{x}) = (2\pi\hbar)^{d/2}\,|\langle\varphi_{\boldsymbol{x}}, \psi_\hbar\rangle|^2\,, \tag{18}$$

where the Gaussian wavepackets $\varphi_{\mathbf{x}} \in L^2(\mathbb{R}^d)$ are defined in (21). This measure can also be obtained by convolution of $\mu^W_{\psi_\hbar}$ with the Gaussian kernel $e^{-|\mathbf{x}-\mathbf{y}|^2/\hbar}$. In these notes our phase space plots show the Husimi measures.

[3] If $\Omega \subset \mathbb{R}^d$ is replaced by a compact riemannian manifold M, we assume that some quantization scheme $f \mapsto \hat{f}_\hbar$ has been developed on $L^2(M)$.

These questions lead us to the notion of phase space localization, or *microlocalization*[4]. We will say that the family of states $(\psi_\hbar)$ is microlocalized inside a set $B \subset T^*\Omega$ if, for *any* smooth observable $f(x,p)$ vanishing near B, the matrix elements $\langle \psi_\hbar, \hat{f}_\hbar \psi_\hbar \rangle$. decrease faster than any power of $\hbar$ when $\hbar \to 0$.

Microlocal properties are not easy to guess from plots of the spatial density $|\psi_j(x)|^2$ like Fig. 1, but they are more natural to study if we want to connect quantum to classical mechanics, since the latter takes place in phase space rather than position space. Indeed, the major tool we will use is the quantum-classical correspondence (4); for all the flows we will consider, any initial spatial test function $f(x)$ evolves into a genuine phase space function $f_t(x,p)$, so a purely spatial formalism is not very helpful. These microlocal properties are easier to visualize on 2-dimensional phase spaces (see below the figures on the 2-torus).

3.1 The case of completely integrable systems

In order to motivate our further discussion of chaotic eigenstates, let us first recall a few facts about the opposite systems, namely completely integrable Hamiltonian flows. For such systems, the energy shell $\mathcal{E}_E$ is foliated by d-dimensional invariant Lagrangian tori. Each such torus is characterized by the values of d independent *invariant actions* $I_1, \ldots, I_d$, so let us call such a torus $T_{\vec{I}}$. The WKB theory allows one to explicitly construct, in the semiclassical limit, precise *quasimodes* of $\hat{H}_\hbar$ associated with some of these tori[5], that is normalized states $\psi_{\vec{I}} = \psi_{\hbar,\vec{I}}$ satisfying

$$\hat{H}_\hbar \, \psi_{\vec{I}} = E_{\vec{I}} \psi_{\vec{I}} + \mathcal{O}(\hbar^\infty), \tag{19}$$

with energies $E_{\vec{I}} \approx E$. Such a Lagrangian (or WKB) state $\psi_{\vec{I}}$ takes the following form (away from caustics):

$$\psi_{\vec{I}}(x) = \sum_{\ell=1}^{L} A_\ell(x;\hbar) \, \exp(iS_\ell(x)/\hbar) \, . \tag{20}$$

Here the functions $S_\ell(x)$ are (local) generating functions[6] for $T_{\vec{I}}$, and each $A_\ell(x;\hbar) = A^0_\ell(x) + \hbar A^1_\ell(x) + \cdots$ is a smooth amplitude.

From this very explicit expression, one can easily check that the state $\psi_{\vec{I}}$ is microlocalized on $T_{\vec{I}}$. On the other hand, our knowledge of $\psi_\hbar$ is much more precise than the latter fact. One can easily construct other states microlocalized on $T_{\vec{I}}$, which are very different from the Lagrangian states $\psi_{\vec{I}}$. For instance, for any point $\mathbf{x}_0 = (x_0, p_0) \in T_{\vec{I}}$ the Gaussian wavepacket (or coherent state)

$$\varphi_{\mathbf{x}_0}(x) = (\pi\hbar)^{-1/4} \, e^{-|x-x_0|^2/2\hbar} \, e^{ip_0 \cdot x/\hbar} \tag{21}$$

is microlocalized on the single point $\mathbf{x}_0$, and therefore also on $T_{\vec{I}}$. This example just reflects the fact that a statement about microlocalization of a sequence of states provides much less information on than a formula like (20).

[4]The prefix *micro* mustn't mislead us: we are still dealing with *macroscopic* localization properties of $\psi_\hbar$!

[5]The "quantizable" tori $T_{\vec{I}}$ satisfy Bohr-Sommerfeld conditions $I_i = 2\pi\hbar(n_i + \alpha_i)$, with $n_i \in \mathbb{Z}$ and $\alpha_i \in [0,1]$ fixed indices.

[6]Above some neighbourhood $U \in \mathbb{R}^d$, the torus $T_{\vec{I}}$ is the union of L lagrangian leaves $\{(x, \nabla S_\ell(x)), \, x \in U\}$, $\ell = 1, \ldots, L$

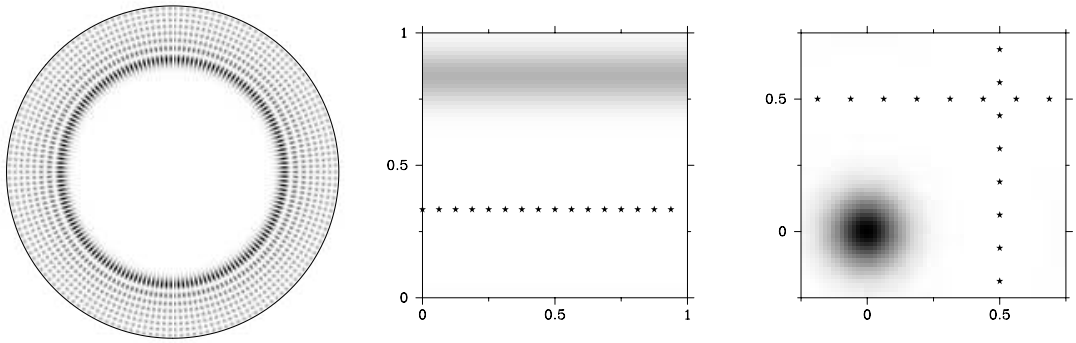

Figure 7: Left: one eigenmode of the circle billiard, microlocalized on a certain torus $T_{\bar{I}}$ (I_1, I_2 can be taken to be the energy and the angular momentum). Center: Husimi density of a simple Lagrangian state on $\mathbb{T}^2$, namely a momentum eigenstate microlocalized on the lagrangian $\{\xi = \xi_0\}$. Right: Husimi density of the Gaussian wavepacket (21). Stars denote the zeros of the Husimi density. (reprinted from [79])

3.2 Quantum ergodicity

In the case of a fully chaotic system, we generally don't have any explicit formula describing the eigenstates, or even quasimodes of $\hat{H}_\hbar$. However, macroscopic informations on the eigenstates can be obtained indirectly, using the quantum-classical correspondence. The main result on this question is a quantum analogue of the ergodicity property (6) of the classical flow, and it is a consequence of this property. For this reason, it has been named *Quantum Ergodicity* by Zelditch. Loosely speaking, this property states that *almost* all eigenstates $\psi_\hbar$ with $E_\hbar \approx E$ will become *equidistributed* on the energy shell $\mathcal{E}_E$, in the semiclassical limit, provided the classical flow on $\mathcal{E}_E$ is ergodic. We give below the version of the theorem in the case of the Laplacian on a compact riemannian manifold, using the notations of (9).

Theorem 1 [Quantum ergodicity] *Assume that the geodesic flow on (M, g) is ergodic w.r.to the Liouville measure. Then, for any orthonormal eigenbasis $(\psi_j)_{j\geq 0}$ of the Laplacian, there exists a subsequence $S \subset \mathbb{N}$ of density 1 (that is, $\lim_{J\to\infty} \frac{\#(S\cap[1,J])}{J} = 1$), such that*

$$\forall f \in C_c^\infty(M), \qquad \lim_{j\in S, j\to\infty} \langle \psi_j, \hat{f}_{\hbar_j} \psi_j \rangle = \int_{\mathcal{E}} f(x,p)\, d\mu_L(x,p)\,,$$

where μ_L is the Liouville measure on $\mathcal{E} = \mathcal{E}_{1/2}$, and $\hbar_j = k_j^{-1}$.

The statement of this theorem was first given by Schnirelman (using test functions $f(x)$) [87], the complete proof was obtained by Zelditch in the case of manifolds of constant negative curvature $\Gamma\backslash\mathbb{H}$ [97], and the general case was then proved by Colin de Verdière [35]. This theorem is "robust": it has been extended to

- quantum ergodic billiards [45, 102]
- quantum Hamiltonians $\hat{H}_\hbar$, such that the flow Φ_H^t is ergodic on $\mathcal{E}_E$ in some energy interval [50]

- quantized ergodic diffeomorphisms on the torus [28] or on more general compact phase spaces [99]
- a general framework of C^* dynamical systems [98]
- a family of quantized ergodic maps with discontinuities [72] and the baker's map [39]
- certain quantum graphs [17]

Let us give the ideas used to prove the above theorem. We want to study the statistical distribution of the matrix elements $\mu_j^W(f) = \langle \psi_j, \hat{f}_{\hbar_j} \psi_j \rangle$ in the range $\{k_j \leq K\}$, with K large. The first step is to estimate the average of this distribution. It is estimated by the generalized Weyl law:

$$\sum_{k_j \leq K} \mu_j(f) \sim \frac{\mathrm{Vol}(M)\sigma_d}{(2\pi)^d} K^d \int_{\mathcal{E}} f \, d\mu_L, \quad K \to \infty \,, \tag{22}$$

where σ_d is the volume of the unit ball in $\mathbb{R}^d$ [53]. In particular, this asymptotics allows to count the number of eigenvalues $k_j \leq K$:

$$\#\{k_j \leq K\} \sim \frac{\mathrm{Vol}(M)\sigma_d}{(2\pi)^d} K^d, \quad K \to \infty, \tag{23}$$

and shows that the average of the distribution $\{\mu_j(f),\, k_j \leq K\}$ converges to the phase space average $\mu_L(f)$ when $K \to \infty$.

Now, we want to show that the distribution is concentrated around its average. This will be done by estimating its variance

$$\mathrm{Var}_K(f) \stackrel{\mathrm{def}}{=} \frac{1}{\#\{k_j \leq K\}} \sum_{k_j \leq K} |\langle \psi_j, (\hat{f}_{\hbar_j} - \mu_L(f))\psi_j \rangle|^2 \,,$$

which has been called the *quantum variance*. Because the ψ_j are eigenstates of $U_\hbar$, we may replace $\hat{f}_{\hbar_j}$ by its quantum time average up to some large time T,

$$\hat{f}_{T,\hbar_j} = \frac{1}{2T} \int_{-T}^{T} U_{\hbar_j}^{-t} \hat{f}_{\hbar_j} U_{\hbar_j}^{-t} \, dt \,,$$

without modifying the matrix elements. At this step, we use the simple inequality

$$|\langle \psi_j, A\psi_j \rangle|^2 \leq \langle \psi_j, A^* A \psi \rangle, \quad \text{for any bounded operator } A,$$

to get the following upper bound for the variance:

$$\mathrm{Var}_K(f) \leq \frac{1}{\#\{k_j \leq K\}} \sum_{k_j \leq K} \langle \psi_j, (\hat{f}_{T,\hbar_j} - \mu_L(f))^* (\hat{f}_{T,\hbar_j} - \mu_L(f))\psi_j \rangle \,.$$

The Egorov theorem (4) shows that the product operator on the right hand side is approximately equal to the quantization of the function $|f_T - \mu_L(f)|^2$, where f_T is the classical time average of f. Applying the generalized Weyl law (22) to this function, we get the bound

$$\mathrm{Var}_K(f) \leq \mu_L(|f_T - \mu_L(f)|^2) + \mathcal{O}_T(K^{-1}) \,.$$

Finally, the ergodicity of the classical flow implies that the function $\mu_L(|f_T - \mu_L(f)|^2)$ converges to zero when $T \to \infty$. By taking T, and then K large enough, the above right hand side can be made arbitrary small. This proves that the quantum variance $Var_K(f)$ converges to zero when $K \to \infty$. A standard Chebychev argument is then used to extract a dense converging subsequence. □

A more detailed discussion on the quantum variance and the distribution of matrix elements $\{\mu_j(f),\, k_j \leq K\}$ will be given in §4.1.3.

3.3 Beyond QE: Quantum Unique Ergodicity vs. strong scarring

3.3.1 Semiclassical measures

Quantum ergodicity can be conveniently expressed by using the concept of *semiclassical measure*. Remember that, using a duality argument, we associate to each eigenstates ψ_j a Wigner distribution μ_j^W on phase space. The quantum ergodicity theorem can be rephrased as follows:

> There exists a density-1 subsequence $S \subset \mathbb{N}$, such that the sequences of Wigner distributions $(\mu_j^W)_{j\in S}$ weak-$*$ (or vaguely) converges to the Liouville measure on $\mathcal{E}$.

For any compact riemannian manifold (M, g), the sequence of Wigner distributions $(\mu_j^W)_{j\in\mathbb{N}}$ remains in a compact set in the weak-$*$ topology, so it is always possible to extract an infinite subsequence $(\mu_j)_{j\in S}$ vaguely converging to a limit distribution μ_{sc}, that is

$$\forall f \in C_c^\infty(T^*M), \quad \lim_{j\in S, j\to\infty} \int f\, d\mu_j^W = \int f\, d\mu_{sc}\,.$$

Such a limit distribution is necessarily a probability measure on $\mathcal{E}$, and is called a *semiclassical measure* of the manifold M. The quantum-classical correspondence implies that μ_{sc} is *invariant* through the geodesic flow: $(\Phi^t)^*\mu_{sc} = \mu_{sc}$. The semiclassical measure μ_{sc} represents the asymptotic (macroscopic) phase space distribution of the eigenstates $(\psi_j)_{j\in S}$. It is the major tool used in the mathematical literature on chaotic eigenstates (see below). The definition can be obviously generalized to any quantized Hamiltonian flow or canonical map.

3.3.2 Quantum Unique Ergodicity conjecture

The quantum ergodicity theorem provides an incomplete information, which leads to the following question:

Question 1 *Do* all *eigenstates become equidistributed in the semiclassical limit? Equivalently, is the Liouville measure the* unique *semiclassical measure for the manifold M? On the opposite, are there* exceptional subsequences *converging to a semiclassical measure $\mu_{sc} \neq \mu_L$?*

This question makes sense if the geodesic flow admits invariant measures different from μ_L (that is, the flow is not uniquely ergodic). Our central example, manifolds of negative curvature, admit many different invariant measures, e.g. the singular measures μ_γ supported on each of the (countably many) periodic geodesics.

This question was already raised in [35], where the author conjectured that no subsequence of eigenstates can concentrate along a single periodic geodesic, that is,

μ_γ cannot be a semiclassical measure. Such an unlikely subsequence was later called a *strong scar* by Rudnick and Sarnak [84], in reference to the *scars* discovered by Heller on the stadium billiard (see §4.2). In the same paper the authors formulated a stronger conjecture:

Conjecture 1 [Quantum unique ergodicity] *Let (M, g) be a compact riemannian manifold with negative sectional curvature. Then all high-frequency eigenstates become equidistributed with respect to the Liouville measure.*

The term *quantum unique ergodicity* refers to the notion of *unique ergodicity* in ergodic theory: a system is uniquely ergodic system if it admits unique invariant probability measure. The geodesic flows we are considering admit many invariant measures, but the conjecture states that the corresponding quantum system selects only one of them.

3.3.3 Arithmetic quantum unique ergodicity

This conjecture was motivated by the following result proved in the cited paper. The authors specifically considered arithmetic surfaces, obtained by quotienting the Poincaré disk $\mathbb{H}$ by certain congruent co-compact groups Γ. As explained in §2.4.2, on such a surface it is natural to consider Hecke eigenstates, which are joint eigenstates of the Laplacian and the (countably many) Hecke operators[7]. It was shown in [84] that any semiclassical measure μ_{sc} associated with Hecke eigenstates does not contain any periodic orbit component μ_γ. The methods of [84] were refined by Bourgain and Lindenstrauss [27], who showed that the measure μ_{sc} of an ϵ-thin tube along any geodesic segment is bounded from above by $C\,\epsilon^{2/9}$. This bound implies that the *Kolmogorov-Sinai entropy* of μ_{sc} is bounded from below by $2/9$[8]. Finally, using advanced ergodic theory methods, Lindenstrauss completed the proof of the QUE conjecture in the arithmetic context.

Theorem 2 [Arithmetic QUE] *[69] Let $M = \Gamma\backslash\mathbb{H}$ be an arithmetic[9] surface of constant negative curvature. Consider an eigenbasis $(\psi_j)_{j\in\mathbb{N}}$ of Hecke eigenstates of $-\Delta_M$. Then, the only semiclassical measure associated with this sequence is the Liouville measure.*

Lindenstrauss and Brooks recently announced an improvement of this theorem: the result holds true, assuming the (ψ_j) are joint eigenstates of Δ_M and of a single Hecke operator T_{n_0}. Their proof uses a new delocalization estimate for regular graphs [30], which replaces the entropy bounds of [27].

This positive QUE result was preceded by a similar statement for the hyperbolic symplectomorphisms on $\mathbb{T}^2$ introduced in §2.5.1. These quantum maps $U_N(S_0)$ have the nongeneric property to be periodic, so one has an explicit expression for their eigenstates. It was shows in [38] that for a certain family hyperbolic matrices S_0 and certain sequences of *prime* values of N, the eigenstates of $U_N(S_0)$ become equidistributed in the semiclassical limit, with an explicit bound on the remainder. Some

[7] The spectrum of the Laplacian on such a surface is believed to be simple; if this is the case, then an eigenstate of Δ is automatically a Hecke eigenstate.

[8] The notion of KS entropy will be further explained in §3.4.

[9] For the precise definition of these surfaces, see [69].

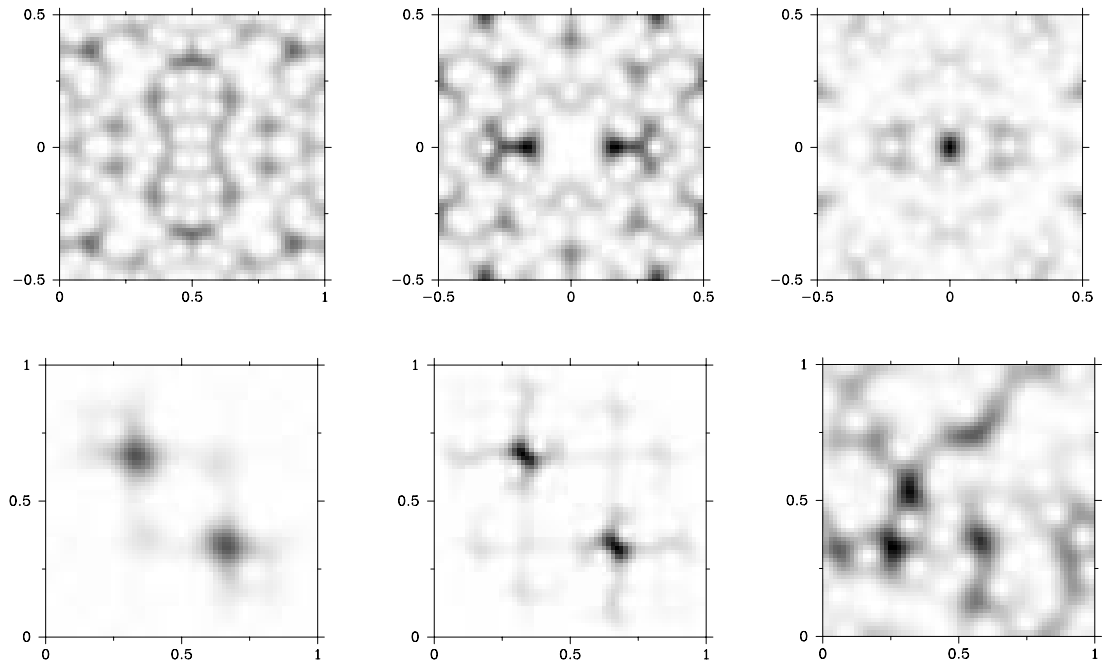

Figure 8: Top: Husimi densities of various states in $\mathcal{H}_N$ (large values=dark regions). Top: 3 (Hecke) eigenstates of the quantum cat map $U_N(S_{DEGI})$, for $N = 107$. Bottom left, center: 2 eigenstates of the quantum baker $U_N(\kappa_B)$ scarred on the period-2 orbit, for $N = 48$ and $N = 128$. Bottom right: random state (35) for $N = 56$. (from [79])

eigenstates, corresponding to the matrix $S_{DEGI} = \begin{pmatrix} 2 & 1 \\ 3 & 2 \end{pmatrix}$ are plotted in Fig. 8, in the Husimi representation.

A few years later, Kurlberg and Rudnick [61] were able to construct, attached to any matrix S_0 and any value of N, a finite commutative family of operators $\{U_N(S'),\ S' \in \mathcal{C}(S_0, N)\}$ including $U_N(S_0)$, which they called "Hecke operators" by analogy with the case of arithmetic surfaces. They then considered specifically the joint ("Hecke") eigenbases of this family, and proved QUE in this framework:

Theorem 3 *[61] Let $S_0 \in SL_2(\mathbb{Z})$ be a quantizable symplectic matrix. For each $N > 0$, consider a Hecke eigenbasis $(\psi_{N,j})_{j=1,\dots,N}$ of the quantum map $U_N(S_0)$. Then, for any observable $f \in C^\infty(\mathbb{T}^2)$ and any $\epsilon > 0$, we have*

$$\langle \psi_{N,j}, \hat{f}_N \psi_{N,j} \rangle = \int f \, d\mu_L + \mathcal{O}_{f,\epsilon}(N^{-1/4+\epsilon}),$$

where μ_L is the Liouville (or Lebesgue) measure on $\mathbb{T}^2$.

As a result, the Wigner distributions of the eigenstates $\psi_{N,j}$ become uniformly equidistributed on the torus, as $N \to \infty$. The eigenstates considered in [38] were instances of Hecke eigenstates.

In view of these positive results, it is tempting to generalize the QUE conjecture to other chaotic systems.

Conjecture 2 [Generalized QUE] *Let Φ_H^t be an ergodic Hamiltonian flow on some energy shell $\mathcal{E}_E$. Then, all eigenstates $\psi_{\hbar,j}$ of $\hat{H}_\hbar$ of energies $E_{\hbar,j} \approx E$ become equidistributed when $\hbar \to 0$.*

Let κ be a canonical ergodic map on $\mathbb{T}^2$. Then, the eigenstates $\psi_{N,j}$ of $U_N(\kappa)$ become equidistributed when $N \to \infty$.

An intensive numerical study for eigenstates of a Sinai-like billiard was carried on by Barnett [15]. It seems to confirm QUE for this system.

In the next subsection we will exhibit particular systems for which this conjecture **fails**.

3.3.4 Counterexamples to QUE: half-scarred eigenstates

In this section we will exhibit sequences of eigenstates converging to semiclassical measures different from μ_L, thus disproving the above conjecture.

Let us continue our discussion of symplectomorphisms on $\mathbb{T}^2$. For any $N \geq 1$, the quantum symplectomorphism $U_N(S_0)$ are periodic (up to a global phase) of period $T_N \leq 3N$, so that its eigenvalues are essentially T_N-roots of unity. For values of N such that $T_N \ll N$, the spectrum of $U_N(S_0)$ is very degenerate, in which case imposing the eigenstates to be of Hecke type becomes a strong requirement. In [62] it is shown that, provided the period is not too small (namely, $T_N \gg N^{1/2-\epsilon}$, which is the case for almost all values of N), then QUE holds for any eigenbasis.

On the opposite, there exist (sparse) values of N, for which the period can be as small as $T_N \sim C \log N$, so that the eigenspaces of huge dimensions $\sim C^{-1} N/\log N$. This freedom allowed Faure, De Bièvre and the author to explicitly construct eigenstates with different localization properties [42, 43].

Theorem 4 *Take $S_0 \in SL_2(\mathbb{Z})$ a (quantizable) hyperbolic matrix. Then, there exists an infinite (sparse) sequence $\mathcal{S} \subset \mathbb{N}$ such that, for any periodic orbit γ of κ_{S_0}, one can construct a sequence of eigenstates $(\psi_N)_{N\in\mathcal{S}}$ of $U_N(S_0)$ associated with the semiclassical measure*

$$\mu_{sc} = \frac{1}{2}\mu_\gamma + \frac{1}{2}\mu_L \,. \tag{24}$$

More generally, for any κ_{S_0}-invariant measure μ_{inv}, one can construct sequences of eigenstates associated with the semiclassical measure

$$\mu_{sc} = \frac{1}{2}\mu_{inv} + \frac{1}{2}\mu_L.$$

This result provided the first counterexample to the generalized QUE conjecture. The eigenstates associated with $\frac{1}{2}\mu_\gamma + \frac{1}{2}\mu_L$ can be called *half-localized*. The coefficient $1/2$ in front of the singular component of μ_γ was shown to be optimal [43], a phenomenon which was then generalized using entropy methods (see §3.4).

Let us briefly explain the construction of eigenstates half-localized on a fixed point $\mathbf{x}_0$. They are obtained by projecting on any eigenspace the Gaussian wavepacket $\varphi_{\mathbf{x}_0}$ (see (21)). Each spectral projection can be expressed as a linear combination of the evolved states $U_N(S_0)^n \varphi_{\mathbf{x}_0}$, for $n \in [-T_N/2, T_N/2 - 1]$. Now, we use the fact that, for N in an infinite subsequence $\mathcal{S} \subset \mathbb{N}$, the period T_N of the operator $U_N(S_0)$ is close to twice the *Ehrenfest time*

$$T_E = \frac{\log \hbar^{-1}}{\lambda}\,, \tag{25}$$

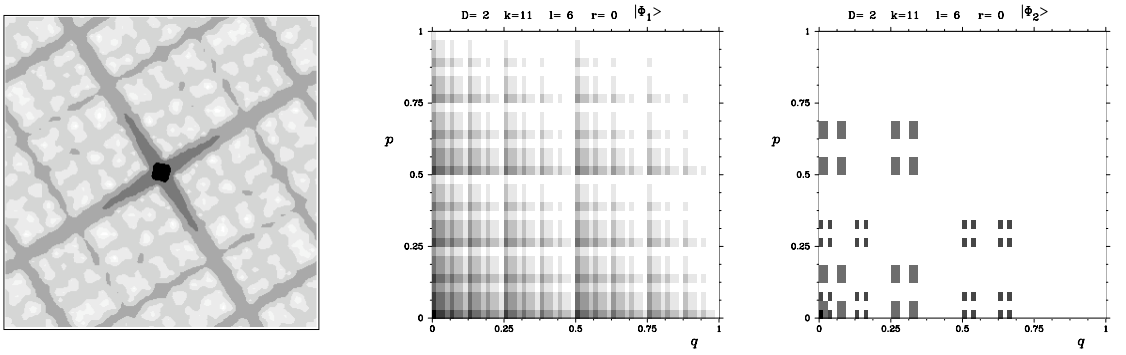

Figure 9: Left: Husimi density of an eigenstate of $U_N(S_{cat})$, strongly scarred at the origin (from [42]). Notice the hyperbolic structure around the fixed point. Center, right: two eigenstates of the Walsh-quantized baker's map (plotted using a "Walsh-Husimi measure"); the corresponding semiclassical measures are fractal (from [2]).

(here λ is the positive Lyapunov exponent). The above linear combination can be split in two components: during the time range $n \in [-T_E/2, T_E/2]$ the states $U_N(S_0)^n \varphi_{\mathbf{x}_0}$ remain microlocalized at the origin; on the opposite, for times $T_E/2 < |n| \leq T_E$, these states expand along long stretches of stable/unstable manifolds, and densely fill the torus. As a result, the sum of these two components is half-localized, half-equidistributed. □

In Fig. 9 (left) we plot the Husimi density associated with one half-localized eigenstate of the quantum cat map $U_N(S_{cat})$.

A nonstandard (Walsh-) quantization of the 2-baker's map was constructed in [2], with properties similar to the above quantum cat map. It allows to exhibit semiclassical measures $\frac{1}{2}\mu_\gamma + \frac{1}{2}\mu_L$ as in the above case, but also purely fractal semiclassical measures void of any Liouville component (see Fig. 9).

Studying hyperbolic toral symplectomorphisms on $\mathbb{T}^{2d}$ for $d \geq 2$, Kelmer [60] identified eigenstates microlocalized on a proper subspace of dimension $\geq d$. He extended his analysis to certain nonlinear perturbations of κ_S. Other very explicit counterexamples to generalized QUE were constructed in [33], based on interval-exchange maps of the interval (such maps are ergodic, but have zero Lyapunov exponents).

3.3.5 Counterexamples to QUE for the stadium billiard

The only counterexample to (generalized) QUE in the case of a chaotic flow concerns the stadium billiard and similar surfaces. This billiard admits a 1-dimensional family of marginally stable periodic orbits, the so-called *bouncing-ball* orbits hitting the horizontal sides of the stadium orthogonally (these orbits form a set of Liouville measure zero, so they do not prevent the flow from being ergodic). In 1984 Heller [51] had observed that some eigenstates are concentrated in the rectangular region (see Fig. 10). These states were baptized *bouncing-ball modes*, and studied quite thoroughly, both numerically and theoretically [52, 9]. In particular, the relative number of these modes becomes negligible in the limit $K \to \infty$, so they are still compatible with quantum ergodicity.

Hassell recently proved [49] that some high-frequency eigenstates of some stadia

indeed fail to equidistribute. To state his result, let us parametrize the shape of a stadium billiard is by the ratio β between the length and the height of the rectangle.

Theorem 5 *[49] For any $\epsilon > 0$, there exists a subset $B_\epsilon \subset [1,2]$ of measure $\geq 1 - 4\epsilon$ and a number $m(\epsilon) > 0$ such that, for any $\beta \in B_\epsilon$, the β-stadium admits a semiclassical measure with a weight $\geq m(\epsilon)$ on the bouncing-ball orbits.*

Although the theorem only guarantees that a fraction $m(\epsilon)$ of the semiclassical measure is localized along the bouncing-ball orbits, numerical studies suggest that the modes are asymptotically fully concentrated on these orbits. Besides, such modes are expected to exist for all ratios $\beta > 0$.

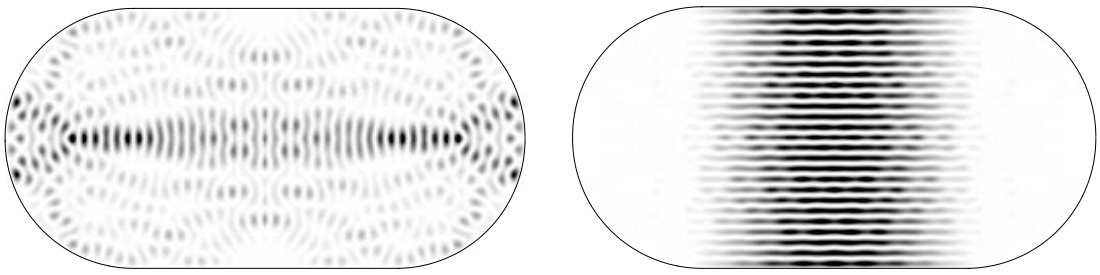

Figure 10: Two eigenstates of the stadium billiard ($\beta = 2$). Left ($k = 39.045$): the mode has a *scar* along the unstable horizontal orbit. Right ($k = 39.292$): the mode is localized in the *bouncing-ball region*.

3.4 Entropy of the semiclassical measures

To end this section on the macroscopic properties, let us mention a recent approach to contrain the possible semiclassical measures occurring in a chaotic system. This approach, initiated by Anantharaman [1], consists in proving nontrivial lower bounds for the *Kolmogorov-Sinai entropy* of the semiclassical measures. The KS (or *metric*) entropy is a common tool in classical dynamical systems, flows or maps [57]. To be brief, the entropy $H_{KS}(\mu)$ of an invariant probability measure μ is a nonnegative number, which quantifies the information-theoretic complexity of μ-typical trajectories. It does not directly measure the localization of μ, but gives some information about it. Here are some relevant properties:

- the delta measure μ_γ on a periodic orbit has entropy zero.
- for an Anosov system (flow or diffeomorphism), the entropy is connected to the unstable Jacobian $J^u(\mathbf{x})$ (see Fig. 3) through the Ruelle-Pesin formula:

$$\text{invariant}, \quad H_{KS}(\mu) \leq \int \log J^u(\rho)\, d\mu,$$

  with equality iff μ is the Liouville measure.
- the entropy is an affine function on the set of probability measures: $H_{KS}(\alpha\mu_1 + (1-\alpha)\mu_2) = \alpha H_{KS}(\mu_1) + (1-\alpha)H_{KS}(\mu_2)$.

In particular, the invariant measure $\alpha\mu_\gamma + (1-\alpha)\mu_L$ of a hyperbolic symplectomorphism S has entropy $(1-\alpha)\lambda$, where λ is the positive Lyapunov exponent.

Anantharaman considered the case of geodesic flows on manifolds M of negative curvature, see §2.4.2. She proved the following constraints on semiclassical measures of M:

Theorem 6 *[1] Let (M,g) be a smooth compact riemannian manifold of negative sectional curvature. Then there exists $c>0$ such that any semiclassical measure μ_{sc} of (M,g) satisfies $H_{KS}(\mu_{sc}) \geq c$.*

In particular, this result forbids semiclassical measures from being supported on unions of periodic geodesics. A more quantitative lower bound was obtained in [2, 4], related with the instability of the flow.

Theorem 7 *[4]Under the same assumptions as above, any semiclassical measure must satisfy*

$$H_{KS}(\mu_{sc}) \geq \int \log J^u \, d\mu_{sc} - \frac{(d-1)\lambda_{\max}}{2}, \tag{26}$$

where $d = \dim M$ and $\lambda_{\max}$ is the maximal expansion rate of the flow.

This lower bound was generalized to the case of the Walsh-quantized baker's map [2], and the hyperbolic symplectomorphisms on $\mathbb{T}^2$ [29, 78], where it takes the form $H_{KS}(\mu_{sc}) \geq \frac{\lambda}{2}$. For these maps, the bound is *saturated* by the half-localized semiclassical measures $\frac{1}{2}(\mu_\gamma + \mu_L)$.

The lower bound (26) is certainly not optimal in cases of variable curvature. Indeed, the right hand side may become negative when the curvature varies too much. A more natural lower bound has been obtained by Rivière in two dimensions:

Theorem 8 *[82, 83]Let (M,g) be a compact riemannian surface of nonpositive sectional curvature. Then any semiclassical measure satisfies*

$$H_{KS}(\mu_{sc}) \geq \frac{1}{2}\int \lambda_+ \, d\mu_{sc}, \tag{27}$$

where λ_+ is the positive Lyapunov exponent.

The same lower bound was obtained by Gutkin for a family of nonsymmetric baker's map [46]; he also showed that the bound is optimal for that system. The lower bound (27) is also expected to hold for ergodic billiards, like the stadium; in particular, it would not contradict the existence of semiclassical measures supported on the bouncing ball orbits.

In higher dimension, one expects the lower bound $H_{KS}(\mu_{sc}) \geq \frac{1}{2}\int \log J^u \, d\mu_{sc}$ to hold for Anosov systems. Kelmer's counterexamples [60] show that this bound may be saturated for certain Anosov diffeomorphisms on $\mathbb{T}^{2d}$.

To close this section, we notice that the QUE conjecture (which remains open) amounts to improving the entropic lower bound (26) to $H_{KS}(\mu_{sc}) \geq \int \log J^u \, d\mu_{sc}$.

4 Statistical description

The macroscopic distribution properties described in the previous section give a poor description of the eigenstates, compared with our knowledge of eigenmodes of

integrable systems. At the practical level, one is interested in quantitative properties of the eigenmodes at finite values of $\hbar$. It is also desirable to understand their structure at the microscopic scale (the scale of the wavelength $R \sim \hbar$), or at least some *mesoscopic* scale ($\hbar \ll R \ll 1$).

The results we will present are of two types. On the one hand, *individual* eigenfunctions will be analyzed statistically, e.g. by computing correlation functions or value distributions of various representations (position density, Husimi). On the other hand, one can also perform a statistical study of a whole bunch of eigenfunctions (around some large wavevector K), for instance by studying how global indicators of localization (e.g. the norms $\|\psi_j\|_{L^p}$) are distributed. We will not attempt to review all possible statistical indicators, but only some "popular" ones.

4.1 Chaotic eigenstates as random states?

It has realized quite early that the statistical data of chaotic eigenstates (obtained numerically) could be reproduced by considering instead ensembles of *random states*. The latter are, so far, the best Ansatz we can find to describe chaotic eigenstates. Yet, one should keep in mind that this Ansatz is of a different type from the WKB Ansatz pointwise describing individual eigenstates of integrable systems. By definition, random states only have a chance to capture the *statistical* properties of the chaotic eigenstates. This "typicality" of chaotic eigenstates should of course be put in parallel with the typicality of spectral correlations, embodied by the Random matrix conjecture (see J.Keating's lecture).

A major open problem in quantum chaos is to prove this "typicality" of chaotic eigenstates. The question seems as difficult as the Random Matrix conjecture.

4.1.1 Spatial correlations

Let us now introduce in more detail the ensembles of random states. For simplicity we consider the Laplacian on a Euclidean planar domain Ω with chaotic geodesic flow (say, the stadium billiard). As in (9), we denote by k_j^2 the eigenvalue of $-\Delta$ corresponding to the eigenmode ψ_j. Let us recall some history.

Facing the absence of explicit expression for the eigenstates, Voros [95, §7] and Berry [18] proposed to (brutally) approximate the Wigner measures μ_j^W of high-frequency eigenstates ψ_j by the Liouville measure μ_L on $\mathcal{E}$. This approximation is justified by the quantum ergodicity theorem, as long as one investigates macroscopic properties of ψ_j. However, the game consisted in also extract some *microscopic* information on ψ_j, so erasing all small-scale fluctuations of the Wigner function could be a dangerous approximation.

Berry [18] showed that this approximation provides nontrivial predictions for the *microscopic correlations* of the eigenstates. Indeed, a partial Fourier transform of the Wigner function leads to the *autocorrelation function* describing the short-distance oscillations of ψ. He defined the correlation function by averaging over some distance R:

$$C_{\psi,R}(x,r) = \overline{\psi^*(x-r/2)\psi(x+r/2)}^R \stackrel{\text{def}}{=} \frac{1}{\pi R^2}\int_{|y-x|\leq R} \psi^*(y-r/2)\psi(y+r/2)\,dy,$$

taking R to be a *mesoscopic scale* $k_j^{-1} \ll R \leq 1$ in order to average over many oscillations of ψ. Inserting μ_L in the place of μ_ψ^W then provides a simple expression

for this function in the range $0 \leq |r| \ll 1$:

$$C_{\psi,R}(x,r) \approx \frac{J_0(k|r|)}{\mathrm{Vol}(\Omega)}\,. \tag{28}$$

Such a homogeneous and isotropic expression could be expected from our approximation. Replacing the Wigner distribution by μ_L suggests that, near each point $x \in \Omega$, the eigenstate ψ is an equal mixture of particles of energy k^2 travelling in all possible directions.

4.1.2 A random state Ansatz

Yet, the approximation μ_L for the Wigner distributions μ_ψ^W is NOT the Wigner distribution of any quantum state[10]. The next question is thus [95]: can one exhibit a family of quantum states whose Wigner measures resemble μ_L? Or equivalently, whose microscopic correlations behave like (28)?

Berry proposed a *random superposition of plane waves* Ansatz to account for these isotropic correlations. One form of this Ansatz reads

$$\psi_{rand,k}(x) = \Big(\frac{2}{N\,\mathrm{Vol}(\Omega)}\Big)^{1/2} \Re\Big(\sum_{j=1}^{N} a_j \exp(k\hat{n}_j \cdot x)\Big)\,, \tag{29}$$

where $(\hat{n}_j)_{j=1,\dots,N}$ are unit vectors distributed on the unit circle, and the coefficients $(a_j)_{j=1,\dots,N}$ are independent identically distributed (i.i.d.) complex normal Gaussian random variables. In order to span all possible velocity directions (within the uncertainty principle), one should include $N \approx k$ directions $\hat{n}_j$ The normalization ensures that $\|\psi_{rand,k}\|_{L^2(\Omega)} \approx 1$ with high probability when $k \gg 1$.

Alternatively, one can replace the plane waves in (29) by circular-symmetric waves, namely Bessel functions. In circular coordinates, the random state reads

$$\psi_{rand,k}(r,\theta) = (\mathrm{Vol}(\Omega))^{-1/2} \sum_{m=-M}^{M} b_m J_{|m|}(kr)\, e^{im\theta}\,, \tag{30}$$

where the coefficients i.i.d. complex Gaussian satisfying the symmetry $b_m = b_{-m}^*$, and $M \approx k$. Both random ensembles asymptotically produce the same statistical results.

The random state $\psi_{rand,k}$ satisfies the equation $(\Delta + k^2)\psi = 0$ in the interior of Ω. Furthermore, $\psi_{rand,k}$ satisfies a "local quantum ergodicity" property: for any observable $f(x,p)$ supported in the interior of $T^*\Omega$, the matrix elements $\langle \psi_{rand,k}, \hat{f}_{k^{-1}} \psi_{rand,k}\rangle \approx \mu_L(f)$ with high probability (more is known about these elements, see §4.1.3).

The stronger claim is that, in the interior of Ω, the *local statistical properties* of $\psi_{rand,k}$, including its microscopic ones, should be similar with those of the eigenstates ψ_j with wavevectors $k_j \approx k$.

The correlation function of eigenstates of chaotic planar billiards has been numerically studied, and compared with this random models, see e.g. [71, 11]. The

[10] Characterizing the function on $T^*\mathbb{R}^d$ which are Wigner functions of individual quantum states is a nontrivial question.

agreement with (28) is fair for some eigenmodes, but not so good for others; in particular the authors observe some anisotropy in the experimental correlation function, which may be related to some form of *scarring* (see §4.2), or to the bouncing-ball modes of the stadium billiard.

The *value distribution* of the random wavefunction (29) is Gaussian, and compares very well with numerical studies of eigenmodes of chaotic billiards [71]. A similar analysis has been performed for eigenstates of the Laplacian on a compact surface of constant negative curvature [6]. In this geometry the random Ansatz was defined in terms of adapted circular hyperbolic waves. The authors checked that the coefficients of the individual eigenfunctions in this expansion were indeed Gaussian distributed; they also checked that the value distribution of individual eigenstates $\psi_j(x)$ is Gaussian to a good accuracy, without any exceptions.

4.1.3 On the distribution of quantum averages

The random state model also predicts the statistical distribution of diagonal matrix elements $\langle \psi_j, \hat{f}_\hbar \psi_j \rangle$, equivalently the average of the observable f w.r.to the Wigner distributions, $\mu_j^W(f)$. The quantum variance estimate in the proof of Thm. 1 shows that the distribution of these averages becomes semiclassically concentrated around the classical value $\mu_L(f)$. Using a mixture of semiclassical and random matrix theory arguments, Feingold and Peres [44] conjectured that, in the semiclassical limit, the matrix elements of eigenstates in a small energy window $\hbar k_j \in [1-\epsilon, 1+\epsilon]$ should be Gaussian distributed, with the mean $\mu_L(f)$ and the (quantum) variance related with the *classical variance* of f. The latter is defined as the integral of the autocorrelation function $C_{f,f}(t)$ (see (7)):

$$\mathrm{Var}_{cl}(f) = \int_{\mathbb{R}} C_{f,f}(t)\, dt\,.$$

A more precise semiclassical derivation [41], using the Gutzwiller trace formula, and supported by numerical computations on several chaotic systems, confirmed both the Gaussian distribution of the matrix elements, and the showed the following connection between quantum and classical variances (expressed in semiclassical notations):

$$\mathrm{Var}_\hbar(f) = g\, \frac{\mathrm{Var}_{cl}(f)}{T_H}\,. \tag{31}$$

Here g is a symmetry factor ($g = 2$ in presence of time reversal symmetry, $g = 1$ otherwise), and $T_H = 2\pi\hbar\bar{\rho}$ is the Heisenberg time, where $\bar{\rho}$ is the smoothed density of states. In the case of the semiclassical Laplacian $-\hbar^2\Delta/2$ on a compact surface or a planar domain, the above right hand side reads $\mathrm{Var}_\hbar(f) = g\hbar\, \mathrm{Var}_{cl}(f)/\,\mathrm{Vol}(\Omega)$. Equivalently, the quantum variance corresponding to wavevectors $k_j \in [K, K+1]$ is predicted to take the value

$$\mathrm{Var}_K(f) \sim \frac{g}{K}\, \frac{\mathrm{Var}_{cl}(f)}{\mathrm{Vol}(\Omega)}\,. \tag{32}$$

Successive numerical studies on chaotic Euclidean billiards [10, 15] and manifolds or billiards of negative curvature [7] globally confirmed this prediction for the quantum

variance, as well as the Gaussian distribution for the matrix elements at high frequency. Still, the convergence to this law can be slowed down for billiards admitting bouncing-ball eigenmodes, like the stadium billiard [10].

For a generic chaotic system, rigorous semiclassical methods could only prove logarithmic upper bounds for the quantum variance [88], $\mathrm{Var}_\hbar(f) \leq C/|\log\hbar|$. Schubert showed that this slow decay can be sharp for certain eigenbases of the quantum cat map, in the case of large spectral degeneracies [89] (as we have seen in §3.3.4, such degeneracies are also responsible for the existence exceptionally localized eigenstates, so a large variance is not surprising).

The only systems for which an algebraic decay is known are of arithmetic nature. Luo and Sarnak [70] proved that, in the case of on the modular domain $M = SL_2(\mathbb{Z})\backslash\mathbb{H}$ (a noncompact, finite volume arithmetic surface), the quantum variance corresponding to high-frequency Hecke eigenfunctions[11] is of the form $\mathrm{Var}_K(f) = \frac{B(f)}{K}$: the polynomial decay is the same as in (32), but the coefficient $B(f)$ is equal the classical variance, "decorated" by an extra factor of arithmetic nature.

More precise results were obtained for quantum symplectomorphisms on the 2-torus. Kurlberg and Rudnick [64] studied the distribution of matrix elements $\{\sqrt{N}\langle\psi_{N,j}, \hat{f}_N\psi_{N,j}\rangle,\ j = 1,\dots,N\}$, where the $(\psi_{N,j})$ form a Hecke eigenbasis of $U_N(S)$ (see §3.3.3). They computed the variance, which is asymptotically of the form $\frac{B(f)}{N}$, with $B(f)$ a "decorated" classical variance. They also computed the fourth moment of the distribution, which suggests that the latter is not Gaussian, but given by a combination of several semi-circle laws on $[-2,2]$ (or Sato-Tate distributions). The same semi-circle law had been shown in [63] to correspond to the asymptotic value distribution of the Hecke eigenstates, at least for N along a subsequence of "split primes".

4.1.4 Maxima of eigenfunctions

Another interesting quantity is the statistics of the maximal values of eigenfunctions, that is their L^∞ norms, or more generally their L^p norms for $p \in (2,\infty]$ (we always assume the eigenfunctions to be L^2-normalized). The maxima belong to the far tail of the value distribution, so their behaviour is a priori uncorrelated with the Gaussian nature of the latter.

The random wave model gives the following estimate [8]: for $C > 0$ large enough,

$$\frac{\|\psi_{rand,k}\|_\infty}{\|\psi_{rand,k}\|_2} \leq C\sqrt{\log k} \quad \text{with high probability when } k \to \infty \tag{33}$$

Numerical tests on some Euclidean chaotic billiards and a surface of negative curvature show that this order of magnitude is correct for chaotic eigenstates [8]. Small variations were observed between arithmetic/non-arithmetic surfaces of constant negative curvature, the sup-norms appearing slightly larger in the arithmetic case, but still compatible with (33). For the planar billiards, the largest maxima occured for states *scarred* along a periodic orbit (see §4.2).

Mathematical results concerning the maxima of eigenstates of generic manifolds of negative curvature are scarce. A general upper bound

$$\|\psi_j\|_\infty \leq C\, k_j^{(d-1)/2} \tag{34}$$

[11] The proof is fully written for the holomorphic cusp forms, but the authors claim that it adapts easily to the Hecke eigenfunctions.

holds for arbitrary compact manifolds [53], and is saturated in the case of the standard spheres. On a manifold of negative curvature, this upper bound can be improved by a logarithmic factor $(log k_j)^{-1}$, taking into account a better bound on the remainder in Weyl's law.

Once again, more precise results have been obtained only in the case of Hecke eigenstates on arithmetic manifolds. Iwaniec and Sarnak [54] showed that, for some arithmetic surfaces, the Hecke eigenstates satisfy the bound

$$\|\psi_j\|_\infty \leq C_\epsilon \, k_j^{5/12+\epsilon} \, ,$$

and conjecture a bound $C_\epsilon \, k_j^\epsilon$, compatible with the random wave model. More recently, Milićević [74] showed that, on certain arithmetic surfaces, a subsequence of Hecke eigenstates satisfies a *lower* bound

$$\|\psi_j\|_\infty \geq C \exp\Big\{ \left(\frac{\log k_j}{\log \log k_j} \right)^{1/2} (1 + o(1)) \Big\} \, ,$$

thereby violating the random wave result. The large values are reached on specific CM-points of the surface, of arithmetic nature.

On higher dimensional arithmetic manifolds, Rudnick and Sarnak [84] had already identified some Hecke eigenstates with larger values, namely

$$\|\psi_j\|_\infty \geq C \, k_j^{1/2} \, .$$

A general discussion of this phenomenon appears in the recent work of Milićević [75]; the author presents a larger family of arithmetic 3-manifolds featuring eigenstate with abnormally large values, and conjectures that his list is exhaustive.

4.1.5 Random states on the torus

In the case of quantized chaotic maps on $\mathbb{T}^2$, one can easily setup a model of random states mimicking the statistics of eigenstates. The choice is particularly when the map does not possess any particular symmetry: the ensemble of random states in $\mathcal{H}_N$ is then given by

$$\psi_{rand,N} = \frac{1}{\sqrt{N}} \sum_{\ell=1}^{N} a_\ell \, e_\ell \, , \tag{35}$$

where $(e_\ell)_{\ell=1,\ldots,N}$ is the orthonormal basis (15) of $\mathcal{H}_N$, and the (a_ℓ) are i.i.d. normal complex Gaussian variables. This random ensemble is $U(N)$-invariant, so it can be defined w.r.to any orthonormal basis of $\mathcal{H}_N$.

This random model, and some variants taking into account symmetries, have been used to describe the spatial, but also the phase space distributions of eigenstates of quantized chaotic maps. In [79], various indicators of localization of the Husimi densities (18) have been computed for this random model, and compared with numerical results for the eigenstates of the quantized "cat" and baker's maps (see Fig. 11). The distributions seem compatible with the random state model, except for the large deviations of the sup-norms of the Husimi densities, due to eigenstates "scarred" at the fixed point $(0, 0)$ (see Fig. 8).

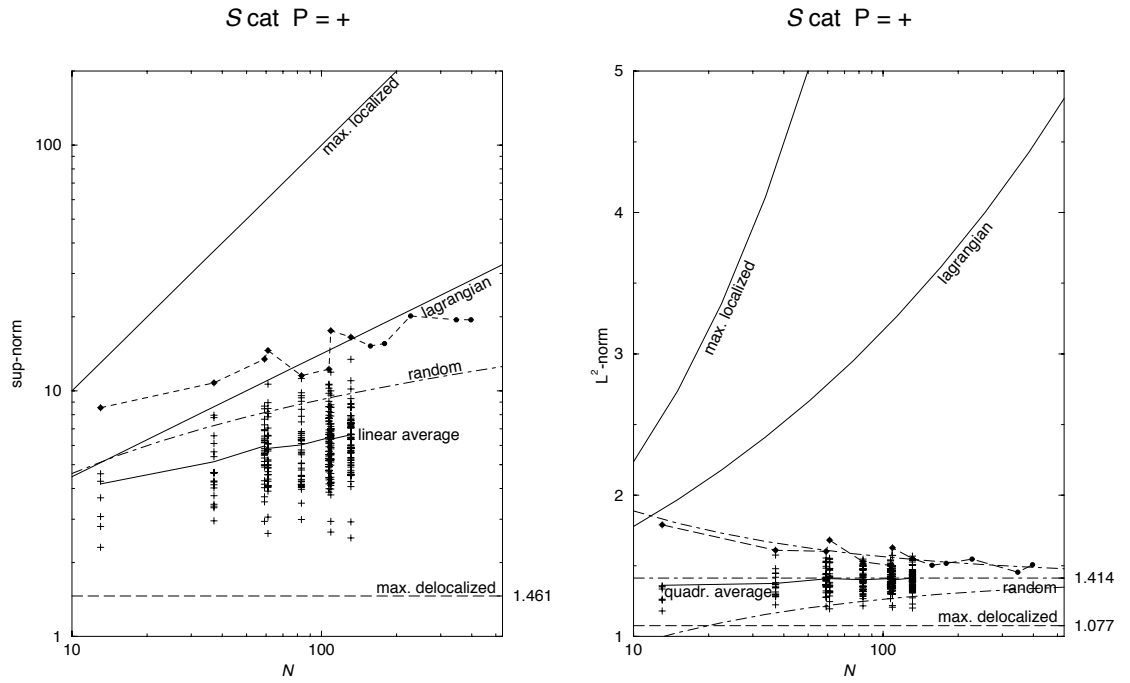

Figure 11: L^∞ (left) and L^2 (right) norms of the Husimi densities for eigenstates of the quantum symplectomorphism $U_N(S_{DEGI})$ (crosses; the dots indicate the states maximally scarred on $(0,0)$). The data are compared with the values for maximally localized states, lagrangian states, random states and the maximally delocalized state. (reprinted from [79]).

In [63] the Hecke eigenstates of $U_N(S)$, expressed as N-vectors in the position basis (e_ℓ), were shown to satisfy nontrivial L^∞ bounds[12]:

$$\|\psi_{N,j}\|_\infty \leq C_\epsilon\, N^{3/8+\epsilon}.$$

Besides, for N along a subsequence of "split primes", the description of the Hecke eigenstates is much more precise. Their position vectors are uniformly bounded, $\|\psi_{N,j}\|_\infty \leq 2$, and the value distribution of individual eigenstates $\{|\psi_{N,j}(\ell/N),\ \ell = 0,\dots,N-1|\}$ is asymptotically given by the semicircle law on $[0,2]$, showing that these eigenstates are very different from Gaussian random states.

In spite of this fact, the value distribution of their Husimi function $\mathbf{x} \to \langle|\varphi_{\mathbf{x}}, \psi_{N,j}\rangle|^2$, which combines $\approx \sqrt{N}$ position coefficients, seems to be exponential.

4.2 Scars of periodic orbits

Around the time the quantum ergodicity theorem was proved, an interesting phenomenon was observed by Heller in numerical studies on the stadium billiard [51]. Heller noticed that for certain eigenfunctions, the spatial density $|\psi_j(x)|^2$ is *abnormally enhanced* along one or several *unstable* periodic geodesics. He called such an enhancement a *scar* of the periodic orbit on the eigenstate ψ_j. See Fig. 10 (left) and Fig. 12 for scars at low and relatively high frequencies.

This phenomenon was observed to persist at higher and higher frequencies for various Euclidean billiards [94, 8], but was not detected on manifolds of negative

[12] In the chosen normalization, the trivial bound reads $\|\psi\|_\infty \leq \|e_\ell\|_\infty = N^{1/2}$.

curvature [6]. Could scarred states represent counterexamples to quantum ergodic-

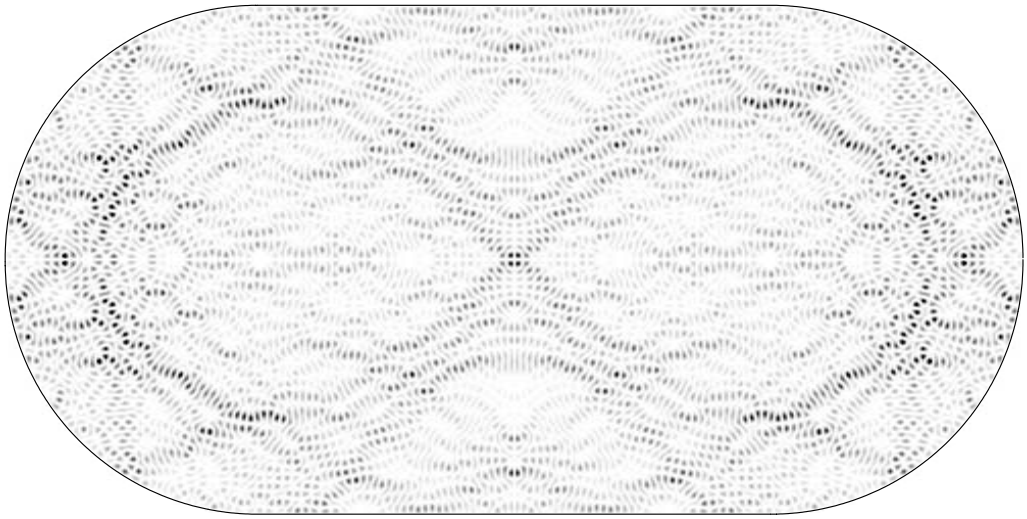

Figure 12: A high-energy eigenmode of the stadium billiard ($k \approx 130$). Do you see any scar?

ity? More precise numerics [15] showed that that the probability weights of these enhancements near the periodic orbits decay in the high-frequency limit, because the *areas* covered by these enhancements decay faster than their *intensities*. As a result, a sequence of scarred states may still become equidistributed in the classical limit [55, 15].

In order to quantitatively characterize the scarring phenomenon, it turned more convenient to switch to phase space representations, in particular the Husimi density of the boundary function $\Psi(q) = \partial_\nu \psi(q)$, which lives on the phase space $T^*\partial\Omega$ of the billiard map [37, 93]. Periodic orbits are then represented by discrete points. Scars were then detected as enhancements of the Husimi density $\mathcal{H}_{\Psi_j}(\mathbf{x})$ on periodic phase space points $\mathbf{x}$.

Similar studies were performed in the case of quantum chaotic maps on the torus, like the baker's map [86] or hyperbolic symplectomorphisms [79]. The scarred state showed in Fig. 8 (left) has the largest value of the Husimi density among all eigenstates of $U_N(S_{DEGI})$, but it is nevertheless a Hecke eigenstate, so that its Husimi measure should be (macroscopically) close to μ_L. This example unambiguously shows that the scarring phenomenon is a microscopic phenomenon, compatible with quantum unique ergodicity.

4.2.1 A statistical theory of scars

Heller first tried to explain the scarring phenomenon using the *smoothed local density of states*

$$S_{\chi,\mathbf{x}_0}(E) = \sum_j \chi(E - E_j) |\langle \varphi_{\mathbf{x}_0}, \psi_j \rangle|^2 = \langle \varphi_{\mathbf{x}_0}, \chi(E - \hat{H}_\hbar) \varphi_{\mathbf{x}_0} \rangle \,, \tag{36}$$

where $\varphi_{\mathbf{x}_0}$ is a Gaussian wavepacket (21) sitting on a point of the periodic orbit; the energy cutoff χ is constrained by the fact that this expression is estimated through

its Fourier transform, that is the time autocorrelation function

$$t \mapsto \langle \varphi_{\mathbf{x}_0}, U_\hbar^t \varphi_{\mathbf{x}_0} \rangle \, \tilde{\chi}(t) \,, \tag{37}$$

where $\tilde{\chi}$ is the $\hbar$-Fourier transform of χ. Because we can control the evolution of $\varphi_{\mathbf{x}_0}$ only up to the Ehrenfest time (25), we must take $\tilde{\chi}$ supported on the interval $[-T_E/2, T_E/2]$, so that χ has width $\gtrsim \hbar/|\log \hbar|$[13].

Since $U_\hbar^t \varphi_{\mathbf{x}_0}$ comes back to the point $\mathbf{x}_0$ at each period T, $S_{\chi,\mathbf{x}}(E)$ has peaks at the *Bohr-Sommerfeld energies* of the orbit, separated by $2\pi\hbar/T$ from one another; however, due to the hyperbolic spreading of the wavepacket, these peaks have widths $\sim \lambda\hbar/T$, where λ is the Lyapunov exponent of the orbit. Hence, the peaks can only be significant for small enough λ, that is weakly unstable orbits. Even if λ is small, the width $\lambda\hbar/T$ becomes much larger than the mean level spacing $1/\bar{\rho} \sim C\hbar^2$ in the semiclassical limit, so that $S_{\chi,\mathbf{x}}(E)$ is a mixture of many eigenstates. In particular, this mechanism can not predict which individual eigenstate will show an enhancement at $\mathbf{x}_0$, nor can it predict the value of the enhancements.

Following Heller's work, Bogomolny [23] and Berry [19] showed that certain linear combinations of eigenstates show some "extra density" in the spatial density (resp. "oscillatory corrections" in the Wigner density) around a certain number of closed geodesics. In the semiclassical limit, these combinations also involve many eigenstates in some energy window.

A decade later, Heller and Kaplan developed a "nonlinear" theory of scarring, which proposes a *statistical* definition of the scarring phenomenon [55]. They noticed that, given an energy interval I of width $\hbar^2 \ll |I| \ll \hbar$, the distribution of the overlaps $\{|\langle \varphi_{\mathbf{x}}, \psi_j \rangle|^2, E_j j \in I\}$ depends on the phase point $\mathbf{x}$: if $\mathbf{x}$ lies on a (mildly unstable) periodic orbit, the distribution is spread between some large values (scarred states) and some low values (antiscarred states). On the opposite, if $\mathbf{x}$ is a "generic" point, the distribution of the overlaps is narrower.

This remark was made quantitative by defining a *stochastic model* for the unsmoothed local density of states $S_{\mathbf{x}}(E)$ (that is, taking χ in (36) to be a delta function), as an effective way to take into account the (uncontrolled) long time recurrences in the autocorrelation function (37). According to this model, the overlaps $\varphi_{\mathbf{x}}, \psi_j\rangle$ in an energy window $I \ni E$ should behave like random Gaussian variables, of *variance given by the smoothed local density* $S_{\chi,\mathbf{x}}(E)$. Hence, if $\mathbf{x}$ lies on a short periodic orbit, the states in energy windows close to the Bohr-Sommerfeld energies (where $S_{\chi,\mathbf{x}}(E)$ is maximal) statistically have larger overlaps with $\varphi_{\mathbf{x}}$, while states with energies E_j close to the anti-Bohr-Sommerfeld energies statistically have smaller overlaps. The concatenation of these Gaussian random variables with smoothly-varying variances produces a non-Gaussian distribution, with a tail larger than the one predicted by Berry's random model. On the opposite, if $\mathbf{x}$ is a "generic" point, the variance should not depend on the energy E_j and the full distribution of the $\varphi_{\mathbf{x}}, \psi_j\rangle$ remains Gaussian.

Although not rigorously justified, this statistical definition of scarring gives quantitative predictions, and can be viewed as an interesting dynamical correction of the random state model (29).

[13] We stick here to 2-dimensional billiards, or maps on $\mathbb{T}^2$, so that the unstable subspaces are 1-dimensional.

5 Nodal structures

After having described the "macroscopic skeleton" of the eigenfunctions ψ_j, namely their semiclassical measures, and the possible large values taken by the ψ_j near a periodic orbit or elsewhere, we now focus on the opposite feature of the ψ_j, namely their *nodal sets*[14] $\mathcal{N}_{\psi_j} = \{x \in \Omega,\, \psi_j(x) = 0\}$. Since the eigenfunctions ψ_j can be chosen real, their nodal set is a union of hypersurfaces (in 2 dimensions, nodal lines), which sometimes intersect each other, or intersect the boundary. This set separates connected domains where ψ_j has a definite sign, called *nodal domains*. The nodal set can be viewed as a *microscopic skeleton* of the eigenfunction ψ_j: it fully determines the function (up to a global factor), and the typical scale separating two nearby hypersurfaces is the wavelength k_j^{-1} (or $\hbar_j$ in the semiclassical formalism).

The study of the nodal patterns of eigenfunctions has a long history in mathematical physics and riemannian geometry. Except for integrable systems[15], we have no explicit knowledge of these sets. However, some global properties are known, independently on any assumption on the geometry. In 1923 Courant [36] showed that, for the Dirichlet Laplacian on a plane domain Ω, the number of nodal domains ν_j of the j-th eigenstate (counted with multiplicities) satisfies $\nu_j \leq j$, an inequality to be compared with the equality valid in 1 dimension. This upper bound was sharpened by Pleijel [81] for high-frequency eigenstates:

$$\limsup_{j\to\infty} \frac{\nu_j}{j} \leq 0.692\,.$$

5.1 Nodal count statistics for chaotic eigenstates

The specific study of nodal structures of eigenstates for *chaotic* billiards is more recent. Blum, Gnutzmann and Smilansky [22] seem to be the first authors to propose using nodal statistics to differentiate regular from chaotic wavefunctions — at least in 2 dimensions. They compared the *nodal count sequence* $(\xi_j = \frac{\nu_j}{j})_{j\geq 1}$ for separable vs. chaotic planar domains, and observed different statistical behaviours. In the separable case the nodal lines can be explicitly computed: they form a "grid", defined in terms of the two independent invariant actions I_1, I_2. The distribution of the sequence is peaked near some value ξ_m depending on the geometry.

In the chaotic case, the authors found that very few nodal lines intersect each other, and conjectured that the sequence should have the same statistics than in the case of the random models (29,30), therefore showing some *universality*. The numerical plot of Fig. 13 perfectly illustrates this assertion. In the random model, the random variable corresponding to $\xi_j = \frac{\nu_j}{j}$ should be

$$\frac{\nu(k)}{\bar{N}(k)}, \qquad k \gg 1\,, \tag{38}$$

where $\nu(k)$ is the number of nodal domains in Ω for the random state (29), and $\bar{N}(k) = \frac{\mathrm{Vol}(\Omega)k^2}{4\pi}$ is the integrated density of states in Ω.

Motivated by these results, Bogomolny and Schmit proposed a *percolation model* to predict the nodal count statistics in random or chaotic wavefunctions [25]. Their

[14] For a moment we will focus on eigenstates of chaotic billiards.

[15] Actually, nodal domains are well-identified only for *separable* systems, a stronger assumption than integrability.

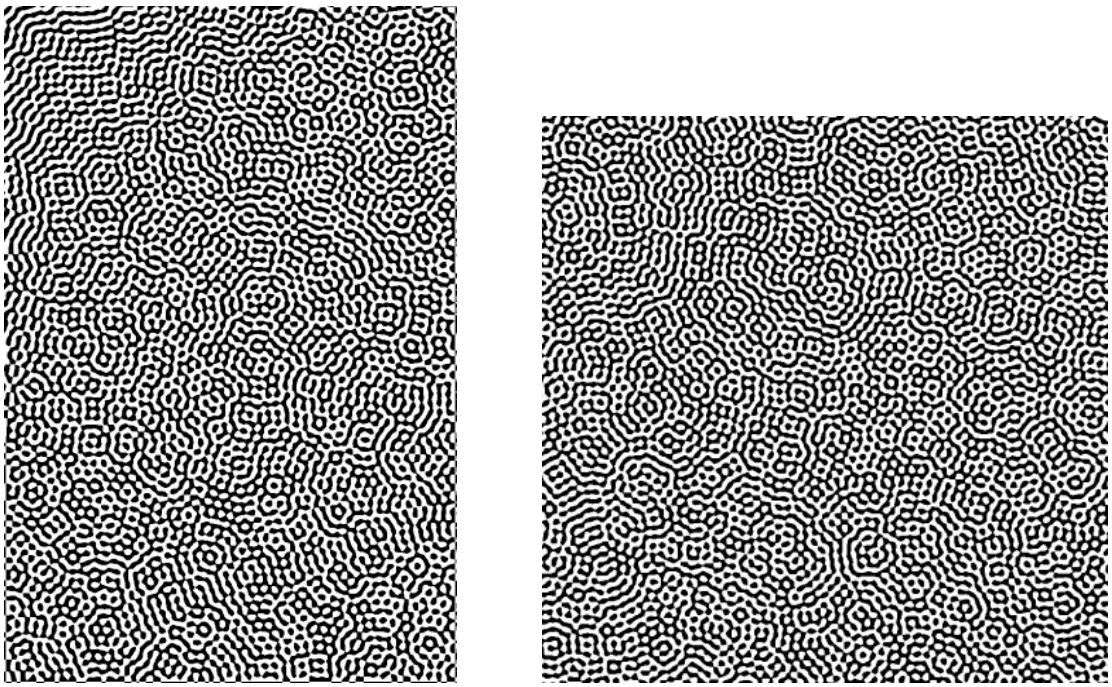

Figure 13: Left: nodal domains of an eigenfunction of the quarter-stadium with $k \approx 100.5$ (do you see the boundary of the stadium?). Right: nodal domains of a random state (30) with $k = 100$ (reprinted from [26]).

model starts from a separable eigenfunction, of the form $\cos(kx/\sqrt{2})\cos(ky/\sqrt{2})$, for which nodal lines form a grid; they perturb this function near each intersection, so that each crossing becomes an avoided crossing (see Fig. 14). Although the length of the nodal set is almost unchanged, the structure of the *nodal domains* is drastically modified by this perturbation. Assuming these local perturbations are *uncorrelated*, they obtain a representation of the nodal domains as *clusters* of a critical bond percolation model, a well-known model in 2-dimensional statistical mechanics.

The (somewhat amazing) claim made in [25] is that such a perturbation of the separable wavefunction has the same nodal count statistics as a random function, eventhough the latter is very different from the former in may ways. This fact can be attributed to the *instability* of the nodal domains of the separable wavefunction (due to the large number of crossings), as opposed to the relative stability of the domains of random states (with generically no crossing). The uncorrelated local perturbations instantaneously transform microscopic square domains into mesoscopic (sometimes macroscopic) "fractal" domains. The high-frequency limit ($k \to \infty$) for the random state (29,30) corresponds to the thermodynamics limit of the percolation model, a limit in which the statistical properties of percolation clusters have been much investigated. The nodal count ratio (39) counts the number of clusters on a lattice of $N_{tot} = \frac{2}{\pi}\bar{N}(k)$ sites. The distribution of the number of domains/clusters $\nu(k)$ was computed in this limit [25]: it is a Gaussian with properties

$$\frac{\langle \nu(k) \rangle}{\bar{N}(k)} \to 0.0624, \qquad \frac{\sigma^2(\nu(k))}{\bar{N}(k)} \to 0.0502\,. \tag{39}$$

Nazarov and Sodin [76] have considered random spherical harmonics on the 2-sphere

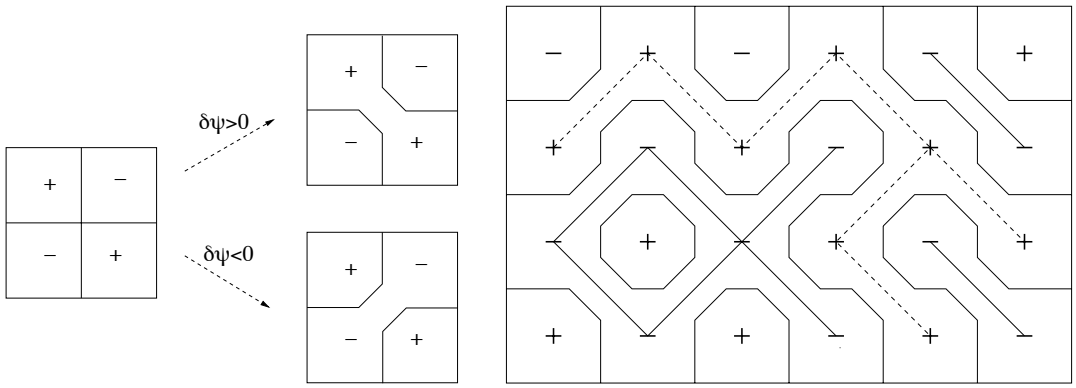

Figure 14: Construction of the random-bond percolation model. Left: starting from a square grid where $\psi(x)$ alternatively takes positive (+) and negative (−) values, a small perturbation $\delta\psi(x)$ near each crossing creates an avoided crossing. Right: the resulting positive and negative nodal domains can be described by setting up bonds (thick/dashed lines) between adjacent sites (reprinted from [25]).

(namely, Gaussian random states within each $2n+1$-dimensional eigenspace, $n \geq 0$), and proved that the number of nodal domains on the eigenspace associated with the eigenvalue $n(n+1)$ statistically behaves like $(a + o(1))n^2$, for some constant $a > 0$. Although they compute neither the constant a, nor the variance of the distribution, this result indicates that the percolation model may indeed correctly predict the nodal count statistics for Gaussian random states.

Remark 2 *We now have* two *levels of modelization. First, the chaotic eigenstates are statistically modelled by the random states (29,30). Second, the nodal structure of random states is modelled by critical percolation. These two conjectures appeal to different methods: the second one is a purely statistical problem, while the first one belongs to the "chaotic=random" meta-conjecture.*

5.2 Other nodal observables

The percolation model also predicts the statistical distribution of the *areas* of nodal domains: this distribution has the form $\mathcal{P}(s) \sim s^{-187/91}$, where s is the area. Of course, this scaling can only hold in the mesoscopic range $k^{-2} \ll s \ll 1$, since any domain has an area $\geq C/k^2$.

The number $\tilde{\nu}_j$ of nodal lines of ψ_j *touching the boundary* $\partial\Omega$ is also an intersting nodal observable. The random state model (30) was used in [22] to predict the following distribution:

$$\frac{\langle \tilde{\nu}(k) \rangle}{k} \xrightarrow{k\to\infty} \frac{\mathrm{Vol}(\partial\Omega)}{2\pi}\,, \qquad \frac{\sigma^2(\tilde{\nu}(k))}{k} \xrightarrow{k\to\infty} 0.0769\ \mathrm{Vol}(\partial\Omega)\,.$$

The same expectation value was rigorously obtained by Toth and Wigman [92], when considering a different random model, namely random superpositions of eigenstates ψ_j of the Laplacian in frequency intervals $k_j \in [K, K+1]$:

$$\psi_{rand,K} = \sum_{k_j \in [K,K+1]} a_j\, \psi_j, \tag{40}$$

with the a_j are i.i.d. normal Gaussians.

5.3 Macroscopic distribution of the nodal set

The volume of the nodal set of eigenfunctions is another interesting quantity. A priori, this volume should be less sensitive to perturbations than the nodal count ν_j. Several rigorous results have been obtained on this matter. Donnelly and Fefferman [40] showed that, for any d-dimensional compact real-analytic manifold, the $(d-1)$-dimensional volume of the nodal set of the Laplacian eigenstates satisfies the bounds

$$C^{-1}\, k_j \,\mathrm{Vol}_{d-1}\,\mathcal{N}(\psi_j) \leq C\, k_j\,,$$

for some $C > 0$ depending on the manifold. The statistics of this volume has been investigated for various ensembles of random states [16, 20, 85]. The average length grows like $c_M\, k$ with a constant $c_M > 0$ depending on the manifold; estimates for the variance are more difficult to obtain. Berry [20] argued that for the 2-dimensional random model (29), the variance should be of order $\log(k)$, showing an unusually strong concentration property for this random variable. Such a logarithmic variance was recently proved by Wigman in the case of random spherical harmonics of the 2-sphere [96].

Counting or volume estimates do not provide any information on the spatial localization of the nodal set. At the microscopic level, Brüning [31] showed that for any compact riemannian manifold, the nodal set $\mathcal{N}(\psi_j)$ is "dense" at the scale of the wavelength: for some constant $C > 0$, any ball $B(x, C/k_j)$ intersects $\mathcal{N}(\psi_j)$.

One can also consider the "macroscopic distribution" of the zero set, by integrating weight functions over the $(d-1)$-dimensional riemannian measure on $\mathcal{N}(\psi_j)$:

$$\forall f \in C^0(M), \qquad \tilde{\mu}^Z_{\psi_j}(f) \stackrel{\mathrm{def}}{=} \int_{\mathcal{N}(\psi_j)} f(x)\, d\,\mathrm{Vol}_{d-1}(x)\,. \tag{41}$$

Similarly with the case of the density $|\psi_j(x)|^2$ or its phase space cousins, the spatial distribution of the nodal set can then be described by the weak-$*$ limits of the renormalized measures $\mu^Z_{\psi_j} = \frac{\tilde{\mu}^Z_{\psi_j}}{\tilde{\mu}^Z_{\psi_j}(M)}$ in the high-frequency limit. In the case of chaotic eigenstates, the following conjecture[16] seems a reasonable "dual" to the QUE conjecture:

Conjecture 3 *Let (M, g) be a compact smooth riemannian manifold, with an ergodic geodesic flow. The, for any orthonormal basis $(\psi_j)_{j\geq 1}$, the probability measures $\mathcal{Z}_{\psi_j}$ weak-$*$ converge to the Lebesgue measure on M, in the limit $j \to \infty$.*

This conjecture is completely open. One slight weakening would be to request that the convergence holds on a density 1 subsequence, as in Thm. 1. Indeed, a similar property can be proved in the complex analytic setting (see §5.5). For M a real analytic manifold, eigenfunctions can be analytically continued in some complex neighbourhood of M, into holomorphic functions $\psi_j^{\mathbb{C}}$. For $(\psi_j)_{j\in S}$ a sequence of ergodic eigenfunctions, Zelditch has obtained the asymptotic distribution of the (complex) nodal set of $\psi_j^{\mathbb{C}}$ [100]; however, his result says nothing about the real zeros (that is, $\mathcal{N}(\psi_j^{\mathbb{C}}) \cap M$).

[16] probably first mentioned by Zelditch

Once more, it is easier to deal with some class of randoms states, than the true eigenstates. In the case of the random spherical harmonics on the sphere, the random ensemble is rotation invariant, so for each level n the expectation of the measures $\mu^Z_{\psi(n)}$ is equal to the (normalized) Lebesgue measure. Zelditch [101] generalized this result to arbitrary compact riemannian manifolds M, by considering random superpositions of eigenstates of the type (40), showing that the expectation of $\mu^Z_{\psi_{rand,K}}$ converges to the Legesgue measure in the semiclassical limit.

The study of nodal sets of random wavefunctions represents lively field of research in probability theory [77].

5.4 Nodal sets for eigenstates of quantum maps on the torus

So far we have only considered the nodal set for the eigenfunctions ψ_j of the Laplacian, viewed in their spatial representation $\psi \in L^2(\Omega)$. These eigenfunctions can be taken real, due to the fact that Δ is a real operator. At the classical level, this reality corresponds to the fact that the classical flow is time reversal invariant.

In the case of quantized maps on the torus with time reversal symmetry, the eigenvectors ψ_j are real elements of $\mathcal{H}_N \equiv \mathbb{C}^N$, with components $\psi_j(\ell/N) = \langle e_\ell, \psi_j \rangle$, $\ell = 0, \ldots, N-1$. Keating, Mezzadri and Monastra [58] defined the nodal domains of such states as the intervals $\{\ell_1, \ell_1 + 1, \ldots, \ell_2 - 1\}$ on which $\psi_j(\ell/N)$ has a constant sign. Using this definition, they computed the exact nodal statistics for a random state (35) (with real Gaussian coefficients a_j), and numerically show that these statistics are satisfied by eigenstates of a generic quantized Anosov map (namely, a perturbation of the symplectomorphism S_{DEGI}).

In a further publication [59], these ideas are extended to canonical maps on the 4-dimensional torus. In this setting, they show that the random state Ansatz directly leads to a percolation model on a triangular lattice, with the same thermodynamical behaviour as the model of [25]. From this remark, they conjecture that, in the appropriate scaling limit, the boundaries of the nodal domains for chaotic eigenstates belong to the universality class of SLE_6 curves, and support this claim by some numerical evidence.

5.5 Husimi nodal sets

The position representation $\psi(x)$ is physically natural, but it is not always the most appropriate to investigate semiclassical properties: phase space representations of the quantum states offer valuable informations, and are more easily compared with invariant sets of the classical flow. We have singled out two such phase space representations: the Wigner function and the Bargmann-Husimi representation. Both can be defined on $T^*\mathbb{R}^d$, but also on the tori $\mathbb{T}^{2d}$. The Wigner function is real and changes sign, so its nodal set is an interesting observable. However, in this section we will focus on the nodal sets of the Husimi (or Bargmann) functions.

The Gaussian wavepackets (21) can be appropriately renormalized into states $\tilde{\varphi}_{\mathbf{x}} \propto \varphi_{\mathbf{x}}$ depending *antiholomorphically* on the complex variable $z = x - ip$. As a result, the Bargmann function associated with $\psi \in L^2(\mathbb{R}^d)$,

$$z \mapsto \mathcal{B}\psi(z) = \langle \varphi_z, \psi \rangle \,,$$

is an entire function of z. For $d = 1$, the nodal set of $\mathcal{B}\psi(z)$ is thus a discrete set of

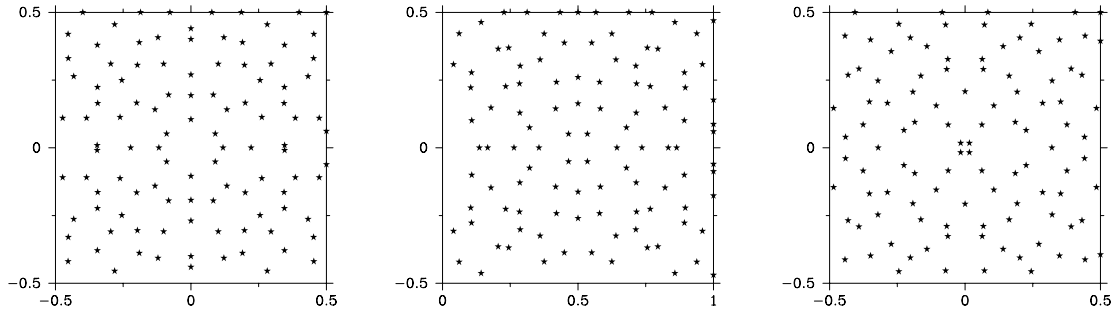

Figure 15: Stellar representation for 3 eigenstates of the quantum cat map $U_N(S_{DEGI})$, the Husimi densities of which were shown in Fig. 8, top, in a *different order*. Can you guess the correspondence?

points in $\mathbb{C}$, which we will denote[17] by $\mathcal{Z}_\psi$. More interestingly, through Hadamard's factorization one can essentially recover the Bargmann function $\mathcal{B}\psi$ from its nodal set, and therefore the quantum state ψ. Assuming $0 \notin \mathcal{Z}_\psi$, we have

$$\mathcal{B}\psi(z) = e^{\alpha z^2+\beta z+\gamma} \prod_{0\neq z_i\in\mathcal{Z}_\psi} (1-z/z_i)\, e^{\frac{z}{z_i}+\frac{1}{2}\frac{z^2}{z_i^2}}\,,$$

leaving only 3 undetermined parameters. Leboeuf and Voros [67] called the set $\mathcal{Z}_\psi$ the *stellar representation* of ψ, and proposed to characterize the chaotic eigenstates using this representation. This idea is especially appealing in the case of a compact phase space like the 2-torus: in that case the Bargmann function $\mathcal{B}\psi$ of a state $\psi_N \in \mathcal{H}_N$ is an entire function on $\mathbb{C}$ satisfying quasiperiodicity conditions, so that its nodal set is $\mathbb{Z}^2$-periodic, and contains exactly N zeros in each fundamental cell. One can then reconstruct the state ψ_N from this set of N points on $\mathbb{T}^2$ (which we denote by $\mathcal{Z}_{\psi_N}^{\mathbb{T}^2}$):

$$\mathcal{B}\psi_N(z) = e^{\gamma} \prod_{z_i\in\mathcal{Z}_{\psi_N}^{\mathbb{T}^2}} \chi(z-z_i)\,,$$

where $\chi(z)$ is a fixed Jacobi theta function vanishing on $\mathbb{Z}+i\mathbb{Z}$. This stellar representation is *exact*, *minimal* (N complex points represent $\psi \in \mathcal{H}_N \equiv \mathbb{C}^N$) and lives in *phase space*. The conjugation of these three properties makes it interesting from a semiclassical point of view.

In [67] the authors noticed a stark difference between the nodal patterns of integrable vs. chaotic eigenstates. In the integrable case, zeros are regularly *aligned along certain curves*, which were identified as anti-Stokes lines in a complex WKB formalism. Namely, the Bargmann function can be approximated by a WKB Ansatz similar with (20) with phase functions $S_j(z)$, and anti-Stokes lines are defined by equations $\Im(S_j(z)-S_k(z))=0$ in regions where $e^{iS_j(z)/\hbar}$ and $e^{iS_k(z)/\hbar}$ dominate the other terms. These curves of zeros are sitting at the "antipodes" of the lagrangian torus where the Husimi density is concentrated (see Fig. 7 (center)).

[17] No confusion will appear between this set and the real nodal sets of the previous section.

On the opposite, the zeros of chaotic eigenstates appear more or less equidistributed across the whole torus (see Fig. 15), like the Husimi density itself. This fact was checked on other systems, e.g. planar billiards, for which the stellar representations of the boundary functions $\partial_\nu \psi_j(x)$ were investigated in [93], leading to similar conclusions. This observation was followed by a rigorous statement, which we express by defining (using the same notation as in the previous section) the "stellar measure" of a state $\psi_N \in \mathcal{H}_N$.

$$\mu^Z_{\psi_N} \stackrel{\text{def}}{=} N^{-1} \sum_{z_i \in \mathcal{Z}^{\mathbb{T}^2}_{\psi_N}} \delta_{z_i} .$$

Theorem 9 *[79] Assume that a sequence of normalized states $(\psi_N \in \mathcal{H}_N)_{N\geq 1}$ becomes equidistributed on $\mathbb{T}^2$ in the limit $N \to \infty$ (that is, their Husimi measures $\mu^H_{\psi_N}$ weak-$*$ converge to the Liouville measure μ_L).*

Then, the corresponding stellar measures $\mu^Z_{\psi_N}$ also weak-$*$ converge to μ_L.

Using the quantum ergodicity theorem (or quantum unique ergodicity when available), one deduces that (almost) all sequences of chaotic eigenstates have asymptotically equidistributed Husimi nodal sets.

This result was proved independently (and in greater generality) by Shiffman and Zelditch [90]. The strategy is to first show that the *electrostatic potential*

$$u_{\psi_N}(\mathbf{x}) = N^{-1} \log \mathcal{H}_{\psi_N}(\boldsymbol{x}) = 2N^{-1} \log |\mathcal{B}\psi_N(z)| - \pi |z|^2$$

decays (in L^1) in the semiclassical limit, and then use the fact that $\mu^Z_{\psi_N} = 4\pi \Delta u_{\psi_N}$. This use of potential theory (specific to the holomorphic setting) explains why such a corresponding statement has not been proved yet for the nodal set of real eigenfunctions (see the discussion at the end of §5.3). To my knowledge, this result is the only rigorous one concerning the stellar representation of chaotic eigenstates.

In parallel, many studies have been devoted to the statistical properties of stellar representation of random states (35), which can then be compared with those of chaotic eigenstates. Zeros of random holomorphic functions (e.g. polynomials) have a long history in probability theory, see e.g. the recent review [77], which mentions the works of Kac, Littlewood, Offord, Rice. The topic has been revived in the years 1990 through questions appearing in quantum chaos [66, 24, 47].

For a Gaussian ensemble like (35), one can explicitly compute the n-point correlation functions of the zeros: besides being equidistributed, the zeros statistically *repel* each other quadratically on the microscopic scale $N^{-1/2}$ (the typical distance between nearby zeros), but are uncorrelated at larger distances. Such a local repulsion (which imposes a certain *rigidity* of random nodal sets) holds in great generality, showing a form of universality at the microscopic scale [21, 77].

The study of [79] suggested that the localization properties of the Husimi measure (e.g. a scar on a periodic orbit) could not be directly visualized in the distribution of the few zeros near the scarring orbit, but rather in the *collective* distribution of all zeros. We thus studied in detail the Fourier coefficients of the stellar measures,

$$\mu^Z_\psi(e^{2i\pi \mathbf{k}\cdot\mathbf{x}}), \qquad 0 \neq \mathbf{k} \in \mathbb{Z}^2 .$$

In the case of the random model (35), the variance of the Fourier coefficients could be explicitly computed: for fixed $\mathbf{k} \neq 0$ and $N \gg 1$, the variance is $\sim \pi^2 \zeta(3) |\mathbf{k}|^4 / N^3$,

showing that typical coefficients are of size $\sim N^{-3/2}$. In the case of chaotic eigenstates, we conjectured an absolute upper bound $o_{\mathbf{k}}(N^{-1})$ for the $\mathbf{k}$-th (the equidistribution of Thm. 9 only forces these coefficients to be $o(1)$). We also argued that the presence of scars in individual eigenfunctions could be detected through the abnormally large values of a few low Fourier modes.

To finish this section, let us mention a few recent rigorous results concerning zeros of random holomorphic functions, after [77]:

- central limit theorems and large deviations of the "linear statistics" $\mu^Z(f)$, with f a fixed test function (including the characteristic function on a bounded domain)
- comparison with other point processes, e.g. the Ginibre ensemble of ensembles of randomly deformed lattices. Here comes the question of the "best matching" of a random zero set (of mean density N) with a square lattice of cell area N^{-1}.
- how to use zero sets to partition the plane into cells.

To my knowledge these properties have not been compared with chaotic eigenstates.

To summarize, the stellar representation provides complementary (*dual*) information to the macroscopic features of the Husimi (or Wigner) measures. The very nonlinear relation with the wavefunction makes its study difficult, but at the same time interesting.

References

[1] N. Anantharaman, *Entropy and the localization of eigenfunctions*, Ann. Math. **168** (2008), 435–475.

[2] N. Anantharaman and S. Nonnenmacher, *Entropy of Semiclassical Measures of the Walsh-Quantized Baker's Map*, Ann. Henri Poincaré **8** (2007), 37–74.

[3] N. Anantharaman and S. Nonnenmacher, *Half–delocalization of eigenfunctions of the laplacian on an Anosov manifold*, Ann. Inst. Fourier **57** (2007), 2465–2523.

[4] N. Anantharaman, H. Koch and S. Nonnenmacher, *Entropy of eigenfunctions*, in *New Trends in Mathematical Physics*, 1–22, V. Sidoravičius (ed.), Springer, Dordrecht, 2009.

[5] D.V. Anosov, *Geodesic flows on closed Riemannian manifolds of negative curvature*, Trudy Mat. Inst. Steklov. **90** (1967).

[6] R. Aurich and F. Steiner, *Statistical properties of highly excited quantum eigenstates of a strongly chaotic system*, Physica **D 64** (1993), 185–214.

[7] R. Aurich and P. Stifter, *On the rate of quantum ergodicity on hyperbolic surfaces and for billiards*, Physica **D 118** (1998), 84–102.

[8] R. Aurich, A. Bäcker, R. Schubert and M. Taglieber, *Maximum norms of chaotic quantum eigenstates and random waves*, Physica **D 129** (1999) 1–14.

[9] A. Bäcker, R. Schubert and P. Stifter, *On the number of bouncing ball modes in billiards*, J. Phys. **A 30** (1997), 6783–6795.

[10] A. Bäcker, R. Schubert and P. Stifter, *Rate of quantum ergodicity in Euclidean billiards*, Phys. Rev. **E 57** (1998) 5425–5447. Erratum: Phys. Rev. **E 58** (1998), 5192.

[11] A. Bäcker and R. Schubert, *Autocorrelation function for eigenstates in chaotic and mixed systems*, J. Phys. **A 35** (2002), 539–564.

[12] N.L. Balasz and A. Voros, *Chaos on the pseudosphere*, Phys. Rep. **143** (1986), 109–240.

[13] N.L. Balasz and A. Voros, *The quantized baker's transformation*, Ann. Phys. (NY) **190** (1989), 1–31.

[14] P. Bàlint and I. Melbourne, *Decay of correlations and invariance principles for dispersing billiards with cusps, and related planar billiard flows*, J. Stat. Phys. **133** (2008), 435–447.

[15] A.H. Barnett, *Asymptotic rate of quantum ergodicity in chaotic Euclidean billiards*, Comm. Pure Appl. Math. *59* (2006), 1457–1488.

[16] P. Bérard, *Volume des ensembles nodaux des fonctions propres du laplacien*, Bony-Sjoestrand-Meyer seminar, 1984–1985, Exp. No. 14, Ecole Polytech., Palaiseau, 1985.

[17] G. Berkolaiko, J.P. Keating and U. Smilansky, *Quantum ergodicity for graphs related to interval maps*, Commun. Math. Phys. **273** (2007), 137–159.

[18] M. V. Berry, *Regular and irregular semiclassical wave functions*, J.Phys. **A, 10** (1977), 2083–91.

[19] M.V. Berry, *Quantum Scars of Classical Closed Orbits in Phase Space*, Proc. R. Soc. Lond. **A 423** (1989), 219–231.

[20] M.V. Berry, *Statistics of nodal lines and points in chaotic quantum billiards: perimeter corrections, fluctuations, curvature*, J. Phys. **A 35** (2002), 3025–3038.

[21] P. Bleher, B. Shiffman and S. Zelditch, *Universality and scaling of correlations between zeros on complex manifolds*, Invent. Math. **142** (2000), 351–395.

[22] G. Blum, S. Gnutzmann and U. Smilansky, *Nodal Domains Statistics: a criterium for quantum chaos*, Phys. Rev. Lett. **88** (2002), 114101.

[23] E.B. Bogomolny, *Smoothed wave functions of chaotic quantum systems*, Physica **D 31** (1988), 169–189.

[24] E. Bogomolny, O. Bohigas and P. Leboeuf, *Quantum chaotic dynamics and random polynomials*, J. Stat. Phys. **85** (1996), 639–679.

[25] E. Bogomolny and C. Schmit, *Percolation model for nodal domains of chaotic wave functions*, Phys. Rev. Lett. **88** (2002), 114102.

[26] E. Bogomolny and C. Schmit, *Random wave functions and percolation*, J. Phys. **A 40** (2007), 14033–14043.

[27] J. Bourgain and E. Lindenstrauss, *Entropy of quantum limits,* Comm. Math. Phys. **233** (2003), 153–171; corrigendum available at `http://www.math.princeton.edu/ elonl/Publications/`.

[28] A. Bouzouina et S. De Bièvre, *Equipartition of the eigenfunctions of quantized ergodic maps on the torus*, Commun. Math. Phys. **178** (1996), 83–105.

[29] S. Brooks, *On the entropy of quantum limits for 2-dimensional cat maps*, Commun. Math. Phys. **293** (2010), 231–255.

[30] S. Brooks and E. Lindenstrauss, *Non-localization of eigenfunctions on large regular graphs*, preprint `arXiv:0912.3239`.

[31] J. Brüning, *Über Knoten von Eigenfunktionen des Laplace-Beltrami-Operators*, Math. Z. **158** (1978), 15–21.

[32] L.A. Bunimovich, *On the ergodic properties of nowhere dispersing billiards*, Commun. Math. Phys. **65** (1979), 295–312.

[33] C-H. Chang, T. Krüger, R. Schubert and S. Troubetzkoy, *Quantisations of Piecewise Parabolic Maps on the Torus and their Quantum Limits*, Commun. Math. Phys. **282** (2008), 395–418.

[34] N. Chernov, *A stretched exponential bound on time correlations for billiard flows*, J. Stat. Phys. **127** (2007) 21-50

[35] Y. Colin de Verdière, *Ergodicité et fonctions propres du Laplacien*, Commun. Math. Phys. **102** (1985), 597–502.

[36] R. Courant and D. Hilbert, *Methoden der mathematischen Physik, Vol. I*, Springer, Berlin, 1931.

[37] B. Crespi, G. Perez and S.-J. Chang, *Quantum Poincaré sections for two-dimensional billiards*, Phys. Rev. *E 47* (1993), 986–991.

[38] M. Degli Esposti, S. Graffi and S. Isola, *Classical limit of the quantized hyperbolic toral automorphisms*, Comm. Math. Phys. **167** (1995), 471–507.

[39] M. Degli Esposti, S. Nonnenmacher and B. Winn, *Quantum variance and ergodicity for the baker's map*, Commun. Math. Phys. **263** (2006), 325–352.

[40] H. Donnelly and C. Fefferman, *Nodal sets of eigenfunctions on Riemannian manifolds*, Invent. Math. **93** (1988), 161–183.

[41] B. Ekhardt *et al.*, *Approach to ergodicity in quantum wave functions*, Phys. Rev. **E 52** (1995), 5893–5903.

[42] F. Faure, S. Nonnenmacher and S. De Bièvre, *Scarred eigenstates for quantum cat maps of minimal periods*, Commun. Math. Phys. **239**, 449–492 (2003).

[43] F. Faure and S. Nonnenmacher, *On the maximal scarring for quantum cat map eigenstates*, Commun. Math. Phys. **245** (2004), 201–214.

[44] M. Feingold and A. Peres, *Distribution of matrix elements of chaotic systems*, Phys. Rev. **A 34** (1986), 591–595.

[45] P. Gérard et G. Leichtnam, *Ergodic properties of eigenfunctions for the Dirichlet problem*, Duke Math. J. **71** (1993), 559–607.

[46] B. Gutkin, *Entropic bounds on semiclassical measures for quantized one-dimensional maps*, Commun. Math. Phys. **294** (2010), 303–342.

[47] J.H. Hannay, *Chaotic analytic zero points: exact statistics for those of a random spin state*, J. Phys. **A 29** (1996), L101–L105.

[48] J. H. Hannay and M. V. Berry, *Quantization of linear maps – Fresnel diffraction by a periodic grating*, Physica **D 1** (1980), 267–290.

[49] A. Hassell, *Ergodic billiards that are not quantum unique ergodic*, with an appendix by A. Hassell and L. Hillairet. Ann. of Math. **171** (2010), 605–618.

[50] B. Helffer, A. Martinez and D. Robert, *Ergodicité et limite semi-classique*, Commun. Math. Phys. **109** (1987), 313–326.

[51] E. J. Heller, *Bound-state eigenfunctions of classically chaotic hamiltonian systems: scars of periodic orbits*, Phys. Rev. Lett. **53** (1984), 1515–1518.

[52] E. J. Heller and P. O'Connor, *Quantum localization for a strongly classically chaotic system*, Phys. Rev. Lett. **61** (1988), 2288–2291.

[53] L. Hörmander, *The spectral function for an elliptic operator*, Acta Math. **127** (1968), 193–218

[54] H. Iwaniec and P. Sarnak, L^∞ norms of eigenfunctions of arithmetic surfaces, Ann. of Math. **141** (1995), 301–320.

[55] L. Kaplan and E.J. Heller, *Linear and nonlinear theory of eigenfunction scars*, Ann. Phys. (NY) **264** (1998), 171–206.

[56] L. Kaplan, *Scars in quantum chaotic wavefunctions*, Nonlinearity **12** (1999), R1–R40.

[57] A. Katok and B. Hasselblatt, *Introduction to the modern theory of dynamical systems*, Cambridge Univ. Press, Cambridge, 1995.

[58] J.P. Keating, F. Mezzadri, and A.G. Monastra, *Nodal domain distributions for quantum maps*, J. Phys. **A 36** (2003), L53–L59.

[59] J.P. Keating, J. Marklof and I.G. Williams, *Nodal domain statistics for quantum maps, percolation, and stochastic Loewner evolution*, Phys. Rev. Lett. **97** (2006), 034101.

[60] D. Kelmer, *Arithmetic quantum unique ergodicity for symplectic linear maps of the multidimensional torus*, Ann. of Math. **171** (2010), 815–879.

[61] P. Kurlberg and Z. Rudnick, *Hecke theory and equidistribution for the quantization of linear maps of the torus*, Duke Math. J. **103** (2000), 47–77.

[62] P. Kurlberg and Z. Rudnick *On quantum ergodicity for linear maps of the torus* Commun. Math. Phys. **222** (2001), 201–227.

[63] P. Kurlberg and Z. Rudnick, *Value distribution for eigenfunctions of desymmetrized quantum maps*, Int. Math. Res. Not. **18** (2001), 985–1002.

[64] P. Kurlberg and Z. Rudnick, *On the distribution of matrix elements for the quantum cat map*, Ann. of Math. **161** (2005), 489–507.

[65] V. F. Lazutkin, KAM theory and semiclassical approximations to eigenfunctions (Addendum by A. Shnirelman), Springer, 1993.

[66] P. Leboeuf and P. Shukla, *Universal tluctuations of zeros of chaotic wavefunctions*, J. Phys. **A 29** (1996), 4827–4835.

[67] P. Leboeuf and A. Voros, *Chaos-revealing multiplicative representation of quantum eigenstates*, J. Phys. **A 23** (1990), 1765–1774.

[68] A.J. Lichtenberg and M.A. Lieberman, *Regular and chaotic dynamics*, 2d edition, Springer, 1992.

[69] E. Lindenstrauss, *Invariant measures and arithmetic quantum unique ergodicity*, Annals of Math. **163** (2006), 165–219.

[70] W. Luo and P.Sarnak, *Quantum variance for Hecke eigenforms*, Ann. Sci. ENS. **37** (2004), 769–799.

[71] S.W. McDonald and A.N. Kaufmann, *Wave chaos in the stadium: statistical properties of short-wave solutions of the Helmholtz equation* Phys. Rev. **A 37** (1988), 3067–3086.

[72] J. Marklof and S. O'Keefe, *Weyl's law and quantum ergodicity for maps with divided phase space*; appendix by S. Zelditch *Converse quantum ergodicity*, Nonlinearity **18** (2005), 277–304.

[73] I. Melbourne, *Decay of correlations for slowly mixing flows*, Proc. London Math. Soc. **98** (2009), 163–190.

[74] D. Milićević, *Large values of eigenfunctions on arithmetic hyperbolic surfaces*, to appear in Duke Math. J.

[75] D. Milićević, *Large values of eigenfunctions on arithmetic hyperbolic 3-manifolds*, preprint.

[76] F. Nazarov and M. Sodin, *On the number of nodal domains of random spherical harmonics*, Amer. J. Math. **131** (2009), 1337–1357.

[77] F. Nazarov and M. Sodin, *Random Complex Zeroes and Random Nodal Lines*, preprint, `arXiv:1003.4237`.

[78] S. Nonnenmacher, *Entropy of chaotic eigenstates*, CRM Proceedings and Lecture Notes **52** (2010), `arXiv:1004.4964`.

[79] S. Nonnenmacher and A. Voros, *Chaotic eigenfunctions in phase space*, J. Stat. Phys. **92** (1998), 431–518.

[80] I. C. Percival, *Regular and irregular spectra*, J. Phys. **B 6** (1973), L229–232.

[81] øA. Pleijel, *Remarks on Courant's nodal line theorem*, Comm. Pure Appl. Math. **8** (1956), 553–550.

[82] G. Rivière, *Entropy of semiclassical measures in dimension 2*, Duke Math. J. (in press), `arXiv:0809.0230`.

[83] G. Rivière, *Entropy of semiclassical measures for nonpositively curved surfaces*, preprint, `arXiv:0911.1840`.

[84] Z. Rudnick and P. Sarnak, *The behaviour of eigenstates of arithmetic hyperbolic manifolds*, Commun. Math. Phys. **161** (1994), 195–213.

[85] Z. Rudnick and I. Wigman, *On the volume of nodal sets for eigenfunctions of the Laplacian on the torus*, Ann. H. Poincaré **9** (2008), 109–130.

[86] M. Saraceno *Classical structures in the quantized baker transformation*, Ann. Phys. (NY) **199** (1990), 37–60.

[87] A. Schnirelman, *Ergodic properties of eigenfunctions*, Uspekhi Mat. Nauk **29** (1974), 181–182.

[88] R. Schubert, *Upper bounds on the rate of quantum ergodicity*, Ann. H. Poincaré **7** (2006), 1085–1098.

[89] R. Schubert, *On the rate of quantum ergodicity for quantised maps*, Ann. H. Poincaré **9** (2008), 1455–1477.

[90] B. Shiffman and S. Zelditch, *Distribution of zeros of random and quantum chaotic sections of positive line bundles*, Commun. Math. Phys. **200** (1999), 661–683.

[91] Ja. G. Sinai, *Dynamical systems with elastic reflections. Ergodic properties of dispersing billiards*, Uspehi Mat. Nauk **25** (1970) no. 2 (152), 141–192.

[92] J. A. Toth and I. Wigman, *Title: Counting open nodal lines of random waves on planar domains*, preprint `arXiv:0810.1276`.

[93] J.-M. Tualle and A. Voros, *Normal modes of billiards portrayed in the stellar (or nodal) representation*, Chaos, Solitons and Fractals **5** (1995), 1085–1102.

[94] E. Vergini and M. Saraceno, *Calculation by scaling of highly excited states of billiards*, Phys. Rev. **E 52** (1995), 2204–2207.

[95] A. Voros, *Asymptotic ħ-expansions of stationary quantum states*, Ann. Inst. H. Poincaré **A 26** (1977), 343–403.

[96] I. Wigman, *Fluctuations of the nodal length of random spherical harmonics*, preprint `0907.1648`.

[97] S. Zelditch, *Uniform distribution of the eigenfunctions on compact hyperbolic surfaces*, Duke Math. J. **55** (1987), 919–941.

[98] S. Zelditch, *Quantum ergodicity of C* dynamical systems*, Commun. Math. Phys. **177** (1996), 507–528.

[99] S. Zelditch, *Index and dynamics of quantized contact transformations*, Ann. Inst. Fourier, **47** (1997), 305–363.

[100] S. Zelditch, *Complex zeros of real ergodic eigenfunctions*, Invent. Math. **167** (2007), 419–443.

[101] S. Zelditch, *Real and complex zeros of Riemannian random waves*, Proceedings of the conference *Spectral analysis in geometry and number theory*, Contemp. Math. **484** 321–342, AMS, Providence, 2009.

[102] S. Zelditch et M. Zworski, *Ergodicity of eigenfunctions for ergodic billiards*, Commun. Math. Phys. **175** (1996), 673–682.